Report of Investigations 2001-1A

BEDROCK GEOLOGIC MAP OF THE CHULITNA REGION, SOUTHCENTRAL ALASKA

by
K.H. Clautice, R.J. Newberry, R.B. Blodgett, T.K. Bundtzen,
B.G. Gage, E.E. Harris, S.A. Liss, M.L. Miller,
R.R. Reifenstuhl, J.G. Clough, and D.S. Pinney

2001

Research supported in part by the U.S. Geological Survey, National Cooperative Geologic Mapping Program, under USGS award number 98HQAG2083. The views and conclusions contained in this document are those of the authors and should not be interpreted as necessarily representing the official policies, either expressed or implied, of the U.S. Government.

STATE OF ALASKA
Tony Knowles, *Governor*

DEPARTMENT OF NATURAL RESOURCES
Pat Pourchot, *Commissioner*

DIVISION OF GEOLOGICAL & GEOPHYSICAL SURVEYS
Milton A. Wiltse, *Director and State Geologist*

Division of Geological & Geophysical Surveys publications can be inspected at the following locations. Address mail orders to the Fairbanks office.

Alaska Division of Geological
& Geophysical Surveys
794 University Avenue, Suite 200
Fairbanks, Alaska 99709-3645

University of Alaska Anchorage Library
3211 Providence Drive
Anchorage, Alaska 99508

Elmer E. Rasmuson Library
University of Alaska Fairbanks
Fairbanks, Alaska 99775-1005

Alaska Resource Library
3150 C Street, Suite 100
Anchorage, Alaska 99503

Alaska State Library
State Office Building, 8th Floor
333 Willoughby Avenue
Juneau, Alaska 99811-0571

This publication released by the Division of Geological & Geophysical Surveys was produced and printed in Fairbanks, Alaska at a cost of $16 per copy. Publication is required by Alaska Statute 41, "to determine the potential of Alaskan land for production of metals, minerals, fuels, and geothermal resources; the location and supplies of groundwater and construction materials; the potential geologic hazards to buildings, roads, bridges, and other installations and structures; and shall conduct such other surveys and investigations as will advance knowledge of the geology of Alaska."

CONTENTS

FIGURES

TABLES

SHEET

[in envelope]

Bedrock geologic map of the Chulitna region, southcentral Alaska

BEDROCK GEOLOGIC MAP OF THE CHULITNA REGION, SOUTHCENTRAL ALASKA

by

K.H. Clautice[1], R.J. Newberry[2], R.B. Blodgett[3], T.K. Bundtzen[4], B.G. Gage[2], E.E. Harris[1], S.A. Liss[1], M.L. Miller[5], R.R. Reifenstuhl[1], J.G. Clough[1], and D.S. Pinney[1]

INTRODUCTION

The Chulitna region is located along Alaska's major railbelt about 150 miles north of Anchorage and hosts the Golden Zone deposit as well as numerous prospects with intriguing values of gold, silver, copper, arsenic, and tin (fig. 1). In an effort to better understand the geology and many known mineral deposits of this area along Alaska's main transportation corridor, a study was initiated by DGGS in 1996 with a 364 mi^2 airborne aeromagnetic and electromagnetic survey (magnetic and resistivity) (DGGS and others, 1997a,b,c,d; Burns, 1997). In 1997, a two-year geologic mapping effort began as follow-up to the airborne geophysical surveys. Because many of the bedrock units in the region have distinctive geophysical signatures, the airborne surveys proved to be extremely useful mapping tools to delineate both map units and structure, particularly in areas of extensive surficial cover. A total of six weeks were spent in the field between 1997 and 1998.

This report includes an interpretive bedrock geologic map (sheet 1) that is based on field observations as well as geophysical interpretation of bedrock contacts in areas of

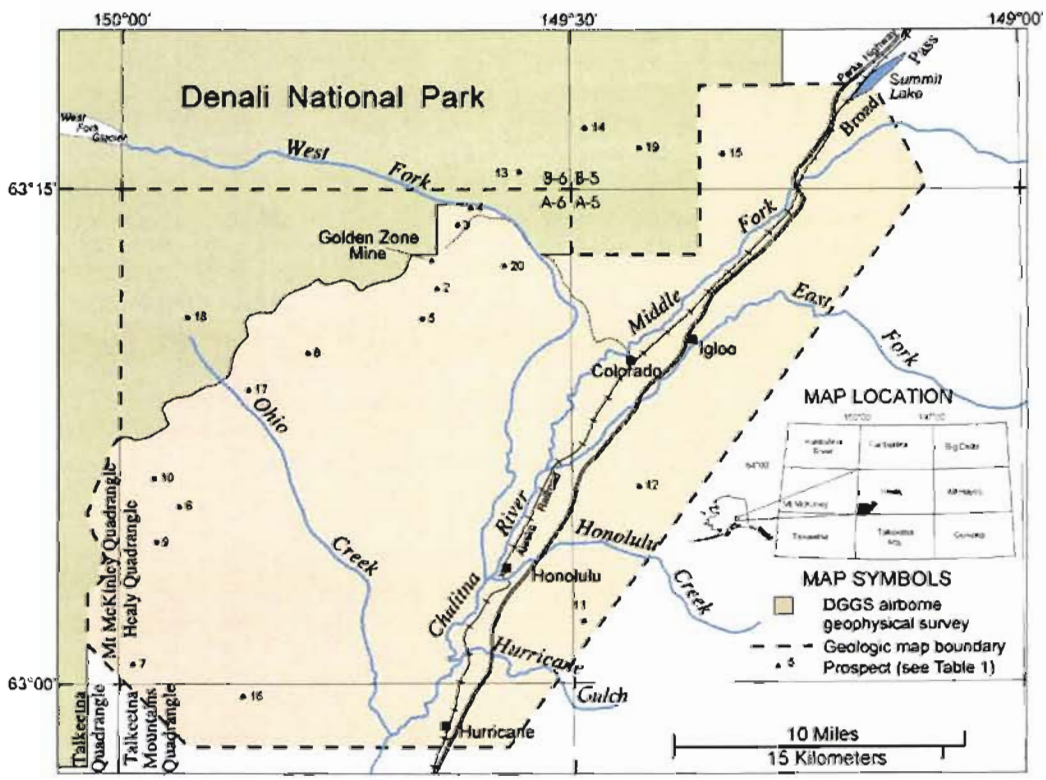

Figure 1. *Chulitna area location map showing selected mineral deposits and prospects (listed in table 1), and boundaries of airborne geophysical survey and geologic mapping.*

[1]Alaska Division of Geological & Geophysical Surveys, 794 University Ave., Suite 200, Fairbanks, Alaska 99709-3645
[2]University of Alaska Fairbanks, Department of Geology & Geophysics, P.O Box 755780, Fairbanks, Alaska 99775-5780
[3]Department o Zoology, Oregon State University, Corvallis Oregon 97331
[4]DGGS at time of field mapping; now with Pacific Rim Geological Consulting, P.O. Box 81906, Fairbanks, Alaska 99708
[5]U.S. Geological Survey, 4200 University Drive, Anchorage, Alaska 99508

surficial cover. The accompanying text includes detailed sections on geochronology, regional structure, economic geology, compositional characteristics of major igneous units, and unit descriptions. The major findings of this study include:

1. Trace element chemistry of the Triassic basalt in Chulitna terrane correlates with that of extensional Late Triassic Nikolai greenstone mapped throughout southern Alaska and contrasts strongly with basalt of similar age from Stikinia terrane.
2. While we recognize some classic redbeds within the Chulitna area, much of what was previously mapped as redbeds has a large volcanic component that chemically resembles calc-alkaline arc rocks.
3. Based on compositional, paleontological, and stratigraphic data, we believe that Chulitna is not a unique terrane as proposed by earlier workers, but is a variant of the Wrangellia terrane of eastern Alaska comprised of Chulitna, West Fork, and Broad Pass terranes (Jones and others, 1981) of earlier usage.
4. Earlier workers (for example, Hawley and Clark, 1973, 1974) postulated two major periods and types of intrusion-related mineralization in the region (older Au–As vs. younger Sn–As). We have documented this age and magmatic distinction and present intrusion- and mineralization-based compositional discriminators for the two major types.
5. We present a stratigraphic and structural model for the district that appears to account for the distribution of mineralization. It consists of a southeast-vergent, tightly folded and commonly overturned stratigraphy cut by north–northeast-trending vertical faults. The intense northeast-trending folding is presumed to be associated with early Late Cretaceous emplacement of the 'Wrangellia' sequence above Jurassic–Cretaceous flysch. Folding and faulting within major blocks provide weakened zones for the emplacement of plutonic-related mineralization; vertical movement between faulted blocks determines the level at which mineralization will be found. For example, down-dropped blocks show little surface expression of mineralization or igneous rock and in places have preserved Tertiary coal beds. Conversely, blocks that display modest 'up' movement contain the Paleozoic and Triassic stratigraphy, vein and breccia deposits, intrusive dikes and plugs, and the majority of the likely intrusion-related mineral resources. Finally, blocks with the greatest amounts of 'up' movement are dominated by the structurally underlying Jurassic and Cretaceous flysch and by extensive exposures of plutonic rocks at levels well below their 'roof' zones. As mineral deposits are largely located in the roof zones of plutons, these deeper-level plutonic exposures are generally unfavorable for intrusion-related mineral deposits.

Additional reports resulting from the Chulitna district study relate to rock chemistry (Gage and others, 1998), comprehensive paleontology (Blodgett and Clautice, 2000), paleomagnetics (Stone and others, 1999), paleontology (Won and others, 2000; Stanley and Yarnell, in press; and Fryda and Blodgett, in press) and stratigraphy (Montayne and Whalen, in press). This report is part of a series (RI 2001-1A-D) which supersedes a series of preliminary maps of the Healy A-6 Quadrangle (the core of the Chulitna region) including interpretive bedrock and geologic maps (Clautice and others, 1999a,b) and Quaternary and engineering geology (Pinney, 1999a,b).

PREVIOUS WORK

Reports by early workers in the district include Brooks and Prindle (1911), Moffit (1915), and Capps (1919, 1940). Ross (1933) recognized fault-controlled mineralization, volcaniclastic rocks, and several major faults. Wahrhaftig (1944) described the area's coal deposits and engineering geology along the nearby Alaska Railroad (Wahrhaftig and Black, 1958). The geology and mineral deposits of the Upper Chulitna district were first described in detail in a series of papers by Hawley and others (1968, 1969), Hawley and Clark (1973, 1974), and Clark and others (1972). Mulligan and others (1967) reported on sampling of the Golden Zone mine, and mineral deposits of the region have been described and sampled by Kurtak and others (1992). Jones and others (1980) mapped (at a scale of 1:63,360) and defined the Chulitna terrane, which they considered to include an ophiolite assemblage, to be one of several allochthonous terranes in the district. Rock ages in their report were established with extensive micro- and macro-fossil identifications. Csejtey and others (1992) published a compilation of the geology of the Healy Quadrangle, which showed the Chulitna district to comprise a series of allochthonous stacked blocks thrust from the north over a basement of Cretaceous melange. Regional geology of southcentral Alaska is summarized in a paper by Nokleberg and others (1994).

REGIONAL GEOLOGY

The Chulitna area is comprised of several northeast-trending belts of rocks of upper Paleozoic to Cretaceous age (herein referred to as the "older assemblage") bounded to both the northwest and southeast by Jurassic to Cretaceous flysch of the Kahiltna assemblage (Reed and Nelson, 1980). Both the Kahiltna and older assemblages are sandwiched between Wrangellia terrane (Jones and others, 1981) to the south and the Denali fault and North America craton or Yukon–Tanana terrane to the north. Published

literature describes much of the Chulitna region as allochthonous terranes most likely accreted to Wrangellia and rafted north to collide with North America in the Late Cretaceous (Csejtey and others, 1992). Based on our mapping and petrology, we suggest instead that Chulitna may be part of Wrangellia and can be correlated with upper Paleozoic to Mesozoic rocks of the east-central Alaska Range and western Yukon Territory, with a complex Cretaceous and younger structural history accompanied by two major intrusive episodes. Our interpretation of the age and character of the units present in the map area (fig. 2) is that they represent only minor modifications of the late Paleozoic to Mesozoic stratigraphy seen throughout southern Alaska, including a mid-Paleozoic oceanic arc, a late Paleozoic to Early Triassic volcanic–sedimentary sequence, a Late Triassic rift-related basalt plus limestone sequence, and a Jurassic–Cretaceous flysch-dominated section. Radiometric age and compositional evidence is provided in this report, paleontologic evidence regarding the possible linkages is found in Blodgett and Clautice (2000).

GEOCHRONOLOGY

METHODS

Twenty-seven rocks from the study area were prepared for $^{40}Ar/^{39}Ar$ dating with monomineralic separates of appropriate K-rich minerals (table 1). After irradiation, the mineral separates were analyzed by step heating, using a 6-watt argon–ion laser, as described in Layer and others (1987). On average, 12–16 fractions were collected for each sample. Samples of hornblende MMhb1 (Samson and Alexander, 1987) with an age of 513.9 Ma were included with each set of unknowns to monitor the neutron flux. Each gas fraction was analyzed for Ar isotopic ratios in a VG-3600 mass spectrometer at the Geophysical Institute, University of Alaska Fairbanks. The argon isotopes measured were corrected for system blank and mass discrimination, as well as calcium, potassium, and chlorine interference. Apparent ages and 1 sigma uncertainties were calculated for each fraction using the constants of Steiger and Jaeger (1977).

Table 1. *Selected mineral deposits and prospects in the Chulitna region. Locations are indicated on figure 1.*

Map no.	Prospect	Longitude	Latitude	Brief description
		I. Mineralization associated with late Cretaceous intrusions		
1	Golden Zone	-149.650	63.214	As-Au-Cu-Ag breccia pipe
2	Copper King	-149.644	63.199	Cu-Au skarn (and porphyry Cu?)
3	Banner	-149.622	63.232	As-Au-Ag skarn
4	Riverside	-149.606	63.240	As-Au-Ag vein and sulfide replacements
5	Long Creek	-149.660	63.184	As-Au-Ag veins and veinlets in hornfels
6	Kennicott	-149.931	63.089	Disseminated sulfides in altered dikes?
7	Eldridge Glacier	-149.983	63.010	Disseminated sulfides in listwanite (quartz-carbonate altered serpentinite) zone
8	Silver Kitty (a)	-149.788	63.166	Au-As intrusive stockwork
	Silver Kitty (b)	-149.788	63.166	Disseminated As-Au-Ag in hornfels near mafic stock
9	Partin Creek	-149.957	63.071	Cu-Au veins, skarns, and carbonate replacements
10	McCallie Glacier Lode	-149.959	63.103	As-Au-Ag veins and sulfide replacements
11	Honolulu	-149.482	63.031	As-Ag-Au vein
12	Antimony	-149.420	63.099	Sb-Au-Ag vein
13	Silver King	-149.553	63.258	As-Au-Ag skarns and veins
14	Nimbus	-149.480	63.280	As-Au-Ag vein and sulfide replacements
15	B-5	-149.327	63.267	As-Au mineralized hornfels zone
		II. Mineralization associated with early Tertiary intrusions		
16	Coal Creek tin	-149.861	62.993	Sn-Ag greisen
17	Ready Cash	-149.854	63.148	Ag-Sn-Zn skarns, sulfide replacements, and veins
18	Ohio Creek	-149.921	63.184	Sn-Ag greisen and minor Zn-Ag skarn
19	Nim	-149.420	63.270	Low-F porphyry Mo (?) and distal veins
20	Lookout Mountain	-149.569	63.211	Distal (?) Sn-Ag tourmaline stockwork

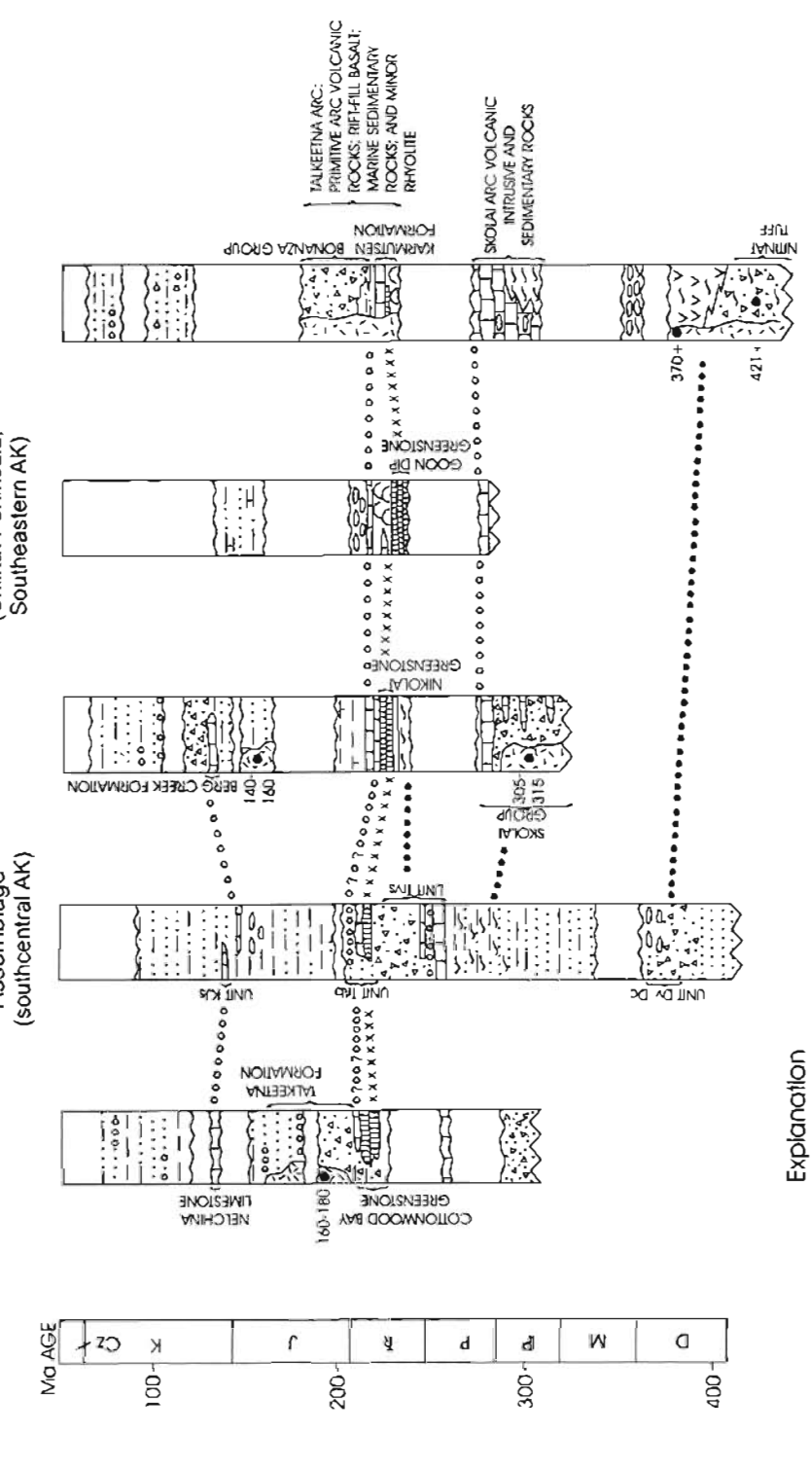

Figure 2. *Diagram illustrating suggested stratigraphic and igneous linkages between Chulitna, Peninsular, and Wrangellia terranes (adapted from Nokleberg and others, 1994) with additions based on data from this study.*

For each sample the "integrated age" (the weighted average of each fraction age) was calculated to facilitate comparison with previously determined K–Ar ages. Where three or more consecutive heating steps yielded the same age (±1 sigma), which accounted for more than 50 percent of the released Ar, the weighted average of these steps was calculated as the "plateau age." Where significant isotopic variations occurred between individual steps, an isochron age was calculated from the $^{40}Ar/^{39}Ar$ and $^{40}Ar/^{36}Ar$ ratios. This age was considered significant only if the Mean Square Weighted Deviation (MSWD) was less than 2.5. For several samples, the last 10 percent or so of gas release yielded an age significantly older than the plateau or isochron age. Because such ages reflect a phase or domain that was less affected by Ar diffusional loss than the bulk of the mineral, they are both indicators of complex thermal history and yield minimum ages of mineral formation. In many such cases, while the Ar spectrum technically satisfied the criteria for a plateau, increasingly older ages for fractions released at increasing temperature ("pseudo plateau") also indicate that the "plateau" age is not a valid measure of the true age.

Lacking anomalous ages for either the higher- or lower-temperature fractions, the interpreted age of the sample was taken to be the isochron (preferred) or plateau age. If neither a plateau nor an isochron (with an MSWD <2.5) could be generated from the step-release heating, then the integrated age was taken as a minimum estimate of the age of mineral formation or re-heating. Where a clearly defined, anomalously old, high-temperature fraction age was determined, this age was taken as a minimum age.

RESULTS

The results of the step-heating Ar measurements, summarized in table 2, indicate that most of the rocks examined experienced complex thermal histories. In particular, all the pre-Jurassic rocks sampled experienced partial to complete Ar loss, indicated by plateau and isochron ages of 145 to 65 Ma (table 2). Because Late Cretaceous igneous rocks are limited to small stocks and dikes, this extensive degree of re-heating *requires* that major igneous bodies of Late Cretaceous age must underlie the Chulitna region. This, in conjunction with the major igneous intrusions in the structural blocks east and west of the Chulitna block, indicates major vertical movements along the high-angle faults bounding the Chulitna block (fig. 3).

The intrusive rock ages also show that some previous age assignments are incorrect. In particular, all mafic intrusions in the region were previously assigned a Tertiary age (Hawley and Clark, 1974); this study (table 2) shows that some are Tertiary (98KC124), some are Late Cretaceous (97RN336), and some are pre-Cretaceous (97RN438). In particular, because pre-Cretaceous mafic intrusions represented by sample 97RN438 (minimum age of 179 Ma) are compositionally indistinguishable from

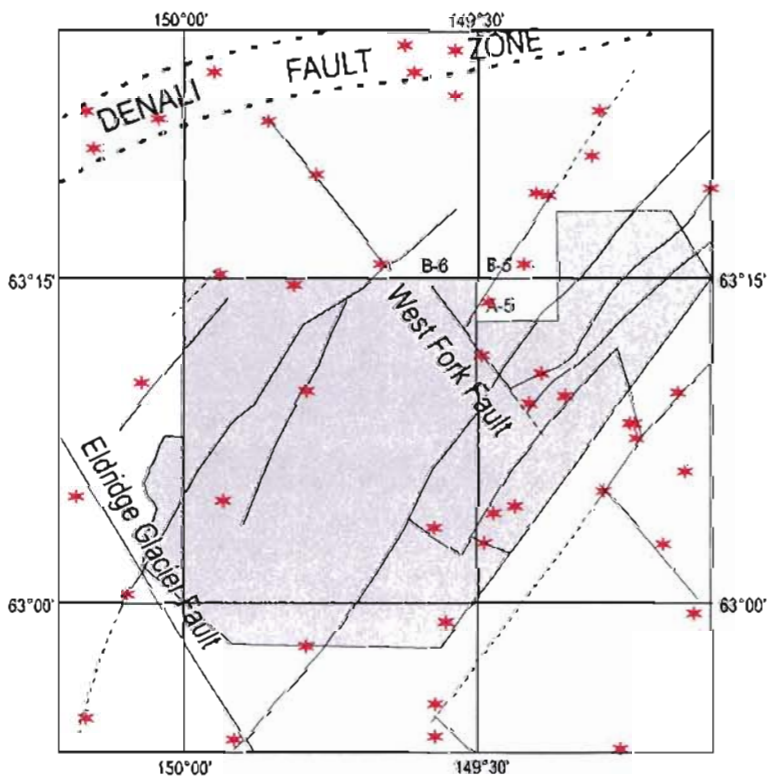

Figure 3. *Simplified structural map of the Chulitna district, showing interpreted high-angle faults and shallow (<20 km) earthquake epicenters (shown as stars) for 1990–1996. Because the earthquake foci are up to 20 km below the surface, and the associated faults have dips of 75–85° (not strictly vertical), a given epicenter can be located up to 5 km down-dip from the surface trace of the associated fault. Earthquake epicenter and focal depth data courtesy of the U.S. Geological Survey, Alaska Earthquake Information Center.*

Table 2. *$^{40}Ar/^{39}Ar$ age data for the Chulitna region*

Sample Number	Unit	Location Longitude	Location Latitude	Rock type	Mineral[b]	Interpreted Age (Ma)[c]	Integrated age (Ma)[d]	Comments[e]
97AM222	uPz?t	-149.658	63.157	Metatuff breccia	Amph	**> 70 ± 1.5 (h)**	61.3 ± 0.5	Pseudo plateau ≈ 65 Ma; reset 35 ± 5 Ma
97BT200	TRvs	-149.646	63.199	Retrograde skarn	Ho	**> 59.9 ± 0.3**	60.2 ± 0.3	Copper King prospect—Good plateau, but Cl/K spectrum suggests reset
97KC281	Km	-149.957	63.071	Quartz monzodiorite	Bi	**67.8 ± 0.3**	67.6 ± 0.3	Partin Creek Prospect—Highest T fraction 70 ± 2 Ma
97KC301	TRs	-150.001	63.049	Quartz diorite dike	Ho	**68.0 ± 0.3**	68.6 ± 0.3	Near Eldridge Glacier prospect—Isochron 67.4 ± 0.3; High T age 74 ± 5 Ma
97KC339	TRs	-149.931	63.089	Altered porphyry dike	WR	**58.6 ± 0.2(I)**	58.6 ± 0.2	Kennicott prospect—Reset ≈ 55 Ma; no plateau or isochron; age probably > 59 Ma
97KC360	TRlb	-149.957	63.071	Altered hornfels	Bi	**75.5 ± 0.4**	67.9 ± 0.4	Partin Creek Prospect—Pseudo plateau, altered spectra, excess age?
					Mu	**70.9 ± 0.5**	67.7 ± 0.6	Partin Creek Prospect—Pseudo plateau; reset at ≈ 30 Ma
97RN330C	TRvs	-149.553	63.258	Skarn	Ho	**63.7 ± 0.3**	63.3 ± 0.4	Silver King—Good plateau; reset at ~ 40 ± 10 Ma Healy B-6
97RN334	K?g	-149.477	63.245	Granite dike	Ksp	**61.4 ± 0.3**	61.5 ± 0.3	Healy B-5, VABM Bull—Good plateau, but Kspar ages are < magmatic age
97RN336	Km	-149.628	63.190	Alkalic? dike	Ho	**66.7 ± 0.9**	68.0 ± 1.1	Good plateau, fair precision
97RN348C	Tg	-149.921	63.184	Greisen	Mu	**55.0 ± 0.2**	55.4 ± 0.3	Ohio Creek prospect—Good plateau
97RN377K	Kg	-149.644	63.199	Altered granite porphyry	Bi	**66.2 ± 0.4**	63.8 ± 0.3	Copper King core—Ar loss ~ 30 Ma, model age ≈ 67 Ma
97RN398	Dv	-149.752	63.131	Meta-andesite flow	Amph	**68 ± 2.4 (i)**	106 ± 9	Secondary (?) actinolitic amphibole; isochron represents reset age
							79.4 ± 1.3	
97RN407D	TRvs	-149.771	63.133	Andesite sill	Pyx	**> 177 (I)**	199 ± 352	Very poor precision; significant Ar loss; isochron at
							177 ± 24	145 ± 15 Ma = reset age?
97RN408B	Km	-149.788	63.166	Diorite pluton	Bi	**> 70.6 ± 1.6 (h)**	66.3 ± 0.3	Silver Kitty Prospect—Pseudo plateau at 66.4 ± 0.3 Ma; high T fraction mostly hornblende
97RN438	TRb	-149.808	63.141	Gabbro body	Pyx	**>179 (I)**	179 ± 7	Ar loss; isochron at 117 ± 5 Ma = reset age?
97RN495C	Km	-149.864	63.120	Biotite diorite	Bi	**66.8 ± 0.3**	66.8 ± 0.3	Good plateau; no loss.
97RN507A	Kg	-149.490	63.016	Granite pluton	Bi + Ho	**>65 ± 0.7 (h)**	51.6 ± 0.7	High T fraction mostly hornblende; Ar loss ≈ 20 Ma; pseudo plateau
							54.6 ± 1.1	at 64.2 ± 1.4 Ma
97RN513A	TRlb	-149.854	63.148	Mineralized hornfels	Ho	**57.6 ± 0.6**	54.8 ± 0.7	Ready Cash—High T fraction 67.7 ± 7.0 Ma; reset 32 Ma
97RR146C	Tg	-149.700	63.147	Granite dike	Bi	**46.0 ± 0.3**	45.9 ± 0.3	Good plateau; no obvious reset
97SL399B	Km	-149.653	63.239	Mafic dike	Ho	**66.8 ± 0.3**	66.9 ± 0.4	Blind Creek—High T fraction 69 ± 4 Ma; slight hump

Sample Number	Unit	Location Longitude	Latitude	Rock type	Mineral[b]	Interpreted Age (Ma)[c]	Integrated age (Ma)[d]	Comments[c]
98BG149	Km	-149.650	63.214	Biotite monzodiorite	Bi	**69.3 ± 0.6**	68.0 ± 0.6	Golden Zone deposit—Model age 69.4 Ma with reset ≈ 23 Ma; similar isochron age
98BG161	Km	-149.650	63.214	Biotite monzodiorite	Bi	**70.1 ± .9 (i)**	67.4 ± 0.6	Golden Zone deposit—Pseudo plateau at 70 ± 0.5 Ma; zero-age reset
98HA11	Kg	-149.486	63.009	Granite chill margin	Bi	**> 71 ± 3 (h)**	49.8 ± 0.4	Healy A-5—Major Ar loss ≈ 16 Ma; pseudo plateau at 66.5 ± 1 Ma
98HA55B	Dv	-149.327	63.267	Hornfelsed volcanic	Bi	**72.7 ± 0.4 (i)**	70.5 ± 0.3	Healy B5, T19S R9W S17—Complex age spectrum; similar plateau age; reset ≈ 25 Ma
98KC124	Tb	-149.483	63.032	Diabase dike	Ho	**52.4 ± 0.2**	51.4 ± 0.2	Healy A-5—Complex spectra: reset = 35–40 Ma
98RN50G	Pl	-149.622	63.231	Skarn	Ho	**69.9 ± 0.9 (i)**	71.1 ± 0.8	Complex age spectrum; similar plateau age
CC36-659	Tg	-149.861	62.993	Sn-greisen	Mu	**53.4 ± 0.2**	53.7 ± 0.2	Talkeetna Mountains D-6, Coal Creek tin deposit—Plateau = isochron age

[a] Analyses performed by P. Layer and J. Drake, University of Alaska Geochronology Laboratory, Geophysical Institute, University of Alaska, Fairbanks, Alaska.
[b] Minerals: Bi = biotite, Ho = hornblende, Amph = low-K amphibole, Pyx = pyroxene, Mu = muscovite (white mica), WR = Whole Rock, Ksp = K-feldspar.
[c] Unless noted otherwise, interpreted ages are plateau ages: I = Integrated age, i = isochron age, h = age of highest-temperature fraction (minimum age). Ages reported at ± 1s.
[d] Equivalent to a conventional K-Ar age, and given for comparison purposes only.

basalt flows interlayered with Late Triassic megafauna (unit TRlb), it is most likely that these intrusions are also of Late Triassic age. Further, since such intrusions are compositionally distinguishable from post-Jurassic ones and intrude unit TRvs ("red beds" of Jones and others, 1980), unit TRvs *must* be older than unit TRlb, and not younger (as inferred by Jones and others, 1980). Such age relationships have vital importance with respect to structural interpretations in the A-6 quadrangle, indicating that many of the thrust faults inferred by Jones and others (1980) are not present.

Tertiary intrusions also caused thermal resets, however, as indicated by disturbances in spectra of several Late Cretaceous plutons and dikes (table 2). Igneous and contact metamorphic rocks from the Partin Creek prospect, for example, yield plateau ages of 76, 71, and 68 Ma. Further, the samples yielding younger plateau ages also gave high-temperature fractions with ages significantly older than the plateau age, indicating post-Cretaceous thermal disturbance. Such results indicate that interpreted ages of Late Cretaceous mineralization and igneous rocks must be viewed with the potential for later thermal resets in mind.

Conventional K–Ar dates previously determined for the large granite intrusion barely in the southeast corner of the A-6 quadrangle indicated an early Tertiary age (Csejtey and others, 1992). Our samples (97RN507, 98HA11; table 2) also yielded early Tertiary integrated (= K–Ar equivalent) ages, but Late Cretaceous pseudo plateau and high-temperature fraction ages indicate the intrusion is instead of Late Cretaceous age. This result has important regional implications, as it demonstrates that not all of the so-called "McKinley age" granites (based on K–Ar ages or general appearance) are of early Tertiary age. Further, since "McKinley age" granites are generally considered favorable for Sn–Ag deposits, but unfavorable for Au deposits (for example, Light and others, 1990) the lode gold potential for the region is likely underestimated.

STRUCTURE

The dominant structures in the Chulitna district are high-angle faults (fig. 3), as indicated by linear patterns of shallow earthquake epicenters. Early workers (for example, Hawley and Clark, 1974) mapped these as high-angle faults because their nearly straight-line surface traces show no deflection by the greater than 2 km topographic relief. Subsequent workers (Jones and others, 1980; Csejtey and others, 1992) mapped these as [moderate- to high-angle] thrust faults to accommodate their geologic model of terrane collision. However, these faults, which can be traced both on the ground and by linear zones of high conductivity, show abrupt breaks on aeromagnetic maps, indicating they are very steeply dipping.

High-angle faults trend mainly northeast, northwest, and north–northeast in the map area. Northeast-trending faults are the most continuous and appear to have the greatest displacement. The northeast faults define the Broad Pass graben and the northwestern margin of the Paleozoic Chulitna) block. We have no direct evidence for the amount of horizontal movement, but the orientation of this northeast-trending fault set suggests that it is related to the Denali fault; thus it may have significant horizontal movement. Vertical displacement of more than a kilometer is suggested by Late Cretaceous and Tertiary plutons, which intrude the Chulitna block (that we believe is in thrust contact above the younger Jurassic–Cretaceous flysch) as high-level dikes and plugs, yet are well exposed and deeply eroded across the northeast bounding faults within Jurassic–Cretaceous flysch.

The second most important fault set is the group containing the northwest-trending faults. They are approximately 20 to 30 km apart and are probably formed as conjugate pairs to the northeast-trending faults. Horizontal and vertical offsets of a few kilometers are likely. Veins and dikes are commonly oriented parallel to the northeast-trending faults, and less commonly parallel to the northwest-trending faults. Such evidence suggests that this faulting began by approximately 70 Ma.

The most abundant faults, but with smallest apparent offset, are the north–northeast-trending set. Earthquake epicenters appear to outline only a few of these (fig. 3), although their topographic expression and minor movement suggest a recent origin. These faults appear to have largely strike-slip movement of less then a few kilometers and truncate against the major, block-defining, northeast-trending faults. A young age is also indicated by the fact that these faults offset veins, skarns, and mineralized Late Cretaceous plutons (sheet 1, photo 1). Tracing mineralization patterns is severely complicated by these younger faults.

Several sets of structures pre-date the high-angle faults; it is difficult to define or trace these older structures. Although there is no direct evidence for low-angle faults in the Chulitna district, indirect evidence suggests that the Paleozoic Chulitna block sits structurally above the extensive Kahiltna assemblage along a low-angle fault surface. The most striking evidence comes from the Late Cretaceous and early Tertiary intrusive rocks in the region. Such intrusions cut all pre-Tertiary rocks in the region, but their outcrop sizes vary dramatically between the major fault blocks. Intrusions with indistinguishable ages and compositions occur as large plutons to batholith-sized bodies in unit KJas, but as dikes or small plugs within the Paleozoic block. Given that the intrusions into KJas commonly occur at higher present elevations than the dikes and plugs in the Chulitna block, these differences can be most readily ascribed to major, post-intrusive uplift of KJas blocks relative to the

Paleozoic blocks. Such a relationship, in turn, requires that the Paleozoic rocks be structurally above KJas, hence in thrust contact.

The major structural style within the Chulitna block is a series of northeast- to north–northeast-plunging, tight, overturned folds, with both limbs dipping to the northwest. Fold wavelength is approximately 1–2 km, and becomes tighter towards the center of the block. Folds in the central part apparently involve the oldest units and are cored by irregular pods of partly serpentinized mafic/ultramafic rocks and serpentinite. Southeast of the strongly folded area are poorly exposed units consisting of weakly metamorphosed tuffs and sediments, within which lack of detailed stratigraphy has not allowed mapping of folds. Similarly, northeast-trending folds were not mapped in the Kahiltna assemblage northwest of the Chulitna block, although the lenticular distribution of subunits is consistent with the presence of relatively tight, commonly isoclinal, folds. This folding most likely accompanied structural emplacement of the Chulitna block, as the folds are cut by undeformed plutons and high-angle faults.

In summary, we infer the structural style of the Chulitna block (units Dv through KJs) to be a tightly folded stratigraphy thrust and overturned toward the south, and subsequently cut by extensive high-angle fault systems Faulting is dominated by a large northeast-trending graben, or down-dropped block, through Broad Pass in which Tertiary gravels have been preserved. Vertical faults parallel to the graben occur on either side of Broad Pass. Vertical movement between northeast-trending blocks controls the erosional level of exposure of mineralizing plutons and thus surface expressions of mineralization in the region.

ECONOMIC GEOLOGY

The only recorded metal production from the Chulitna district is from the Golden Zone deposit (fig. 1). Between 1941 and 1942 it produced 1,581 oz Au, 8,617 oz Ag, 21 tons Cu, and 1.5 tons Pb (figs. 4 and 5). A small amount of placer gold was mined from Bryn Mawr Creek, immediately downstream from the Golden Zone, and from McCallie Creek, in the western part of the quadrangle. Field descriptions and assay data for major prospects are given in Hawley and Clark (1974), Kurtak and others (1992), and Gage and others (1998).

Stratiform, syngenetic/diagenetic deposits appear to be rare or nonexistent in the Chulitna district. Although volcanic rocks that evidently erupted into aqueous environments are common in the A-6 quadrangle, there is no evidence for submarine hydrothermal activity or volcanogenic massive sulfide deposits. Because the Permo–Triassic unit (TRvs) formerly referred to as "sedimentary redbeds" (Jones and others, 1980) consists principally of iron-rich, mafic volcaniclastic rocks and associated sediments, and is not a "redbed" in the commonly accepted sense of a hematitic sandstone, there is no likelihood of redbed-associated Cu deposits in this unit. Basalt-hosted and basalt-associated Cu deposits, which are

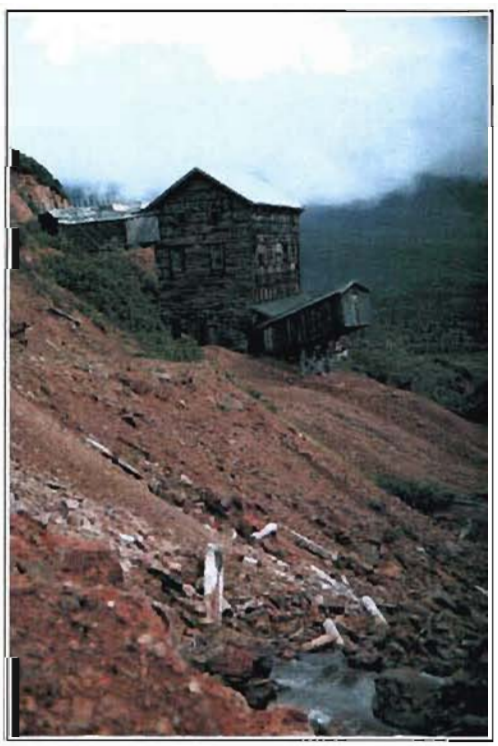

Figure 4 (left). *The Golden Zone Mine mill, which was built in 1939–40 and in use during 1941–42, when the Golden Zone produced 1,581 oz Au, 8,617 oz Ag, 21 tons Cu, and about 3,000 lb Pb from 1,730 tons of ore (Hawley and Clark, 1974) (1997 photo by M.L. Miller).*

Figure 5 (below). *C.C. Hawley showing M.L. Miller the contact between the ore body breccia (below) and the strongly jointed Cretaceous monzonite, (unit Km, above) at the Golden Zone Mine (photo by K.H. Clautice).*

common in—and stratigraphically above—Late Triassic basalts elsewhere in the northwest Cordillera, are only present in areas with thick accumulations of subaerial basalt (MacKevett and others, 1997). As the equivalent basalt units in the A-6 quadrangle are thin and interbedded with carbonate rocks, this mineralization style is also unlikely in the area. Placer gold accumulations are not significant, as the area has been eroded by multiple glaciation events in the recent past.

Very small bodies of chromite are present within serpentinite in at least two locations in the A-6 quadrangle (Hawley and Clark, 1974). Neither occurrence is of significant size, and given the extremely discontinuous and faulted nature of the serpentinite bodies, there is limited likelihood for a large chromite accumulation in the quadrangle. Although small amounts of disseminated or veinlet pyrite have been noted in some altered gabbroic rocks of the region, no magmatic sulfides have been identified, and no significant Cu–Ni or platinum-group metal anomalies have been found in the mafic intrusions (Hawley and Clark, 1974; Kurtak and others, 1992; Gage and others, 1998).

The majority of known mineral resources in the Chulitna district (table 1) are spatially and temporally (table 2) associated with Cretaceous and Tertiary age intermediate to felsic intrusions. Although the various prospects and deposits possess similarities, those associated with Late Cretaceous intrusions are fundamentally different from those with early Tertiary intrusions. The former contain significant Au resources and the latter significant Ag–Sn. Hawley and Clark (1974) drew similar conclusions, but regarded all the intermediate-composition intrusions as older, Au-related, and all the felsic-composition intrusions (including Cretaceous granite types) as younger, Sn related. In many cases the two deposit types are difficult to distinguish. Arsenopyrite and pyrite are characteristic minerals of both types and anomalous concentrations of Sn, Bi, Te, and Au can be found in either type (Hawley and Clark, 1974; Warner and Dahlin, 1989; Kurtak and others, 1992; Gage and others, 1998). Empirically, however,

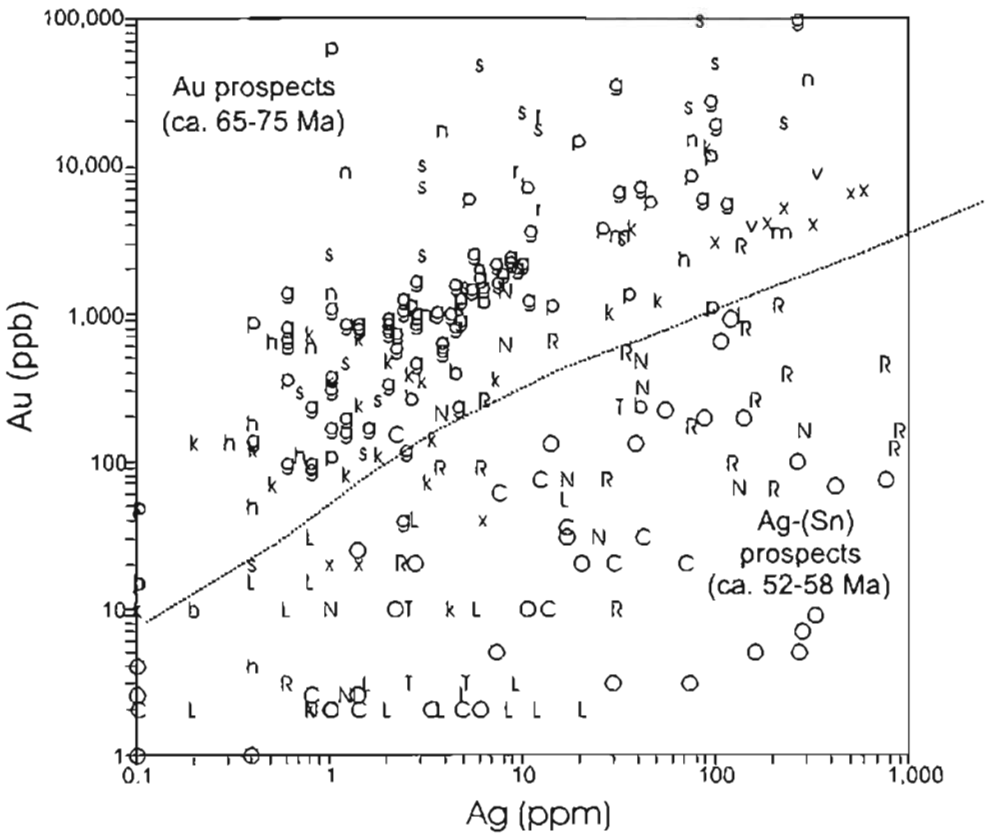

Figure 6. *Concentrations of silver vs. gold in mineralized samples from the Chulitna area. Prospect abbreviations: Golden Zone and nearby prospects = g, Riverside = r, East Vein = v, Banner (skarn) = b, Copper King = k, Silver King = s, Long Creek = x, Honolulu = h, Nim = n, Partin Creek = p, McCallie Glacier = m, Lookout Mountain = L, Ohio Creek = O, Coal Creek = C, Ready Cash = R, Nimbus = N, and other early Tertiary-type prospects = T. Data from Hawley and Clark (1974), Warner and Dahlin (1989), Kurtak (1992), Newberry (1995), and Gage and others (1998).*

the two types can be distinguished by their Au and Ag contents: the Ag/Au ratios are invariably higher in most hand samples from the Sn–Ag type than in hand samples from the Au type (fig. 6). When broken into these two types, based on Au and Ag contents, interpreted minimum $^{40}Ar/^{39}Ar$ ages for mineralized and associated rocks mostly fall into two groups: 65–75 Ma for the Au type and 52–58 Ma for the Sn–Ag type (fig. 7). Thermal resetting of some older mineralization by early Tertiary dikes and intrusions appears to account for the majority of overlap between the two types.

Plutonic-related vein/breccia gold deposits in the region are exemplified by the Golden Zone deposit (Hawley and Clark, 1974). These deposits are spatially associated with reduced (low primary magnetite) granitic rocks ranging from intermediate to felsic compositions. The ores contain abundant arsenopyrite, pyrite, and commonly pyrrhotite, with lesser stibnite and/or antimony–sulfosalts, molybdenite, bismuthinite, Bi–Te–S minerals, and minor to trace scheelite, consistent with a reduced environment of formation (McCoy and others, 1997). Stannite is present in trace amounts. Gangue minerals include major quartz, very fine- to coarse-grained white mica, calcite, and ferroan dolomite. Given this mineralogy, the geochemical expression is Au–As–Bi–Sb–Te (Zn,Cu,Ag,B,Sn,Be).

Skarns and sulfide replacement bodies (table 1) are present where carbonate-bearing rocks occur near mineralized Early Cretaceous plutons. Although they commonly contain abundant chalcopyrite, their high Au/Ag ratios, abundant arsenopyrite, and high Bi contents indicate most are better classified as "gold skarns" than as "copper skarns" (Meinert, 1992; Newberry and others, 1997). Within the study area there are commonly some gold-bearing veins in the Au-rich skarns, and some small amounts of skarn with the pluton-hosted veins/breccias, but the two deposit types appear to be largely mutually exclusive. Although high-carbonate rocks are the best host rocks, appreciable amounts of skarn are present in units with as little as 10 percent carbonate (for example, TRvs). The largest example is at Silver King (Hawley and Clark, 1974,

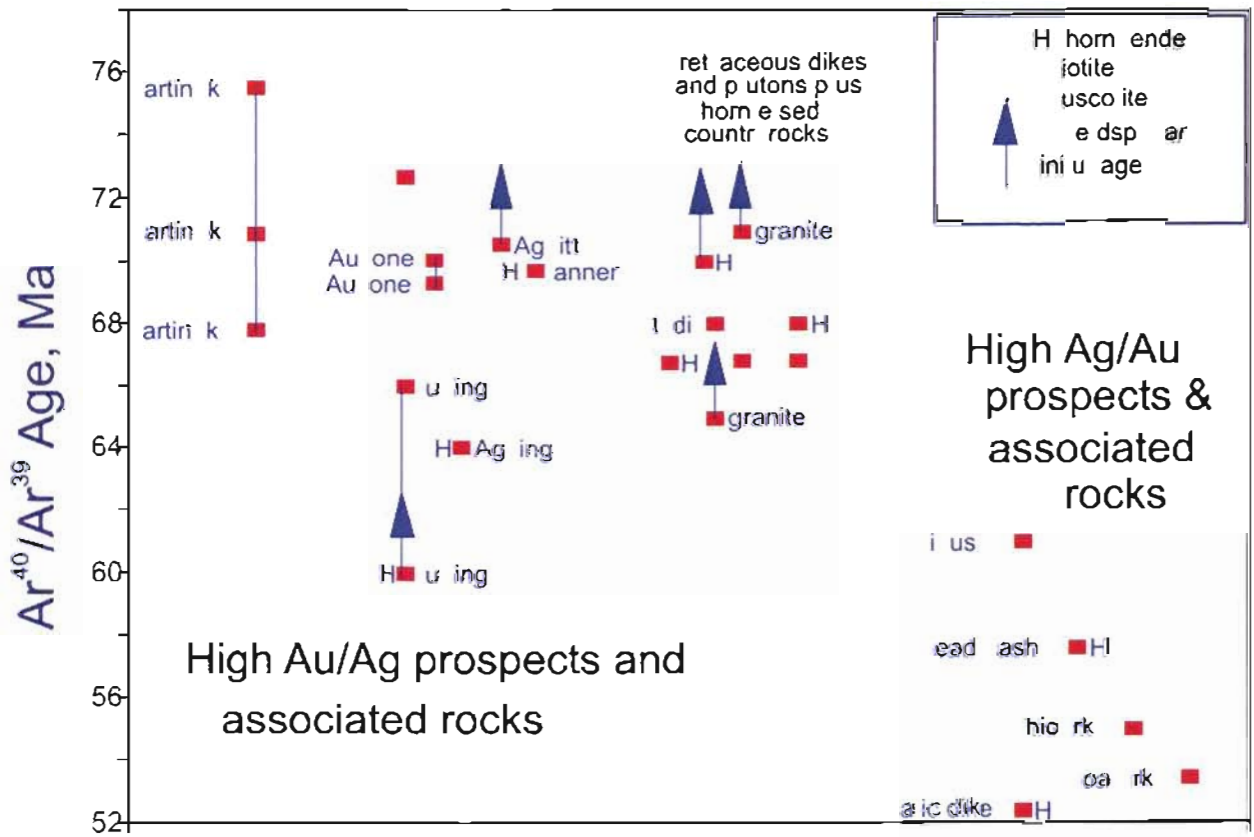

Figure 7. *Interpreted $^{40}Ar/^{39}Ar$ ages for mineralized and related rocks in the Chulitna region, taken from table 1. Vertical arrows designate age from highest-temperature Ar fraction and indicate minimum age; all other ages are from $^{40}Ar/^{39}Ar$ plateau. Vertical lines connect samples from the same prospect. Note the clear age separation between those prospects (fig. 6) characterized by lower Ag/Au ratios (approximately 65–75 Ma) and those characterized by high Ag/Au ratios. Except for Nimbus, a weakly mineralized porphyry Mo prospect of uncertain age, the high Ag/Au deposits all contain appreciable Sn. Data from this study.*

Newberry and others, 1997) immediately north of the Healy A-6 Quadrangle.

These Au-rich skarns contain pyrite, magnetite, chalcopyrite, arsenopyrite ± pyrrhotite as the dominant sulfides; small to trace amounts of bornite, molybdenite, scheelite, and Bi–Te minerals are also present (Newberry, 1995). The most common gangue minerals are low-Fe garnet, high-Fe clinopyroxene, hornblende, calcite, and quartz. The geochemical signature for these deposits is: Cu–Ag–Au–Bi–As–Sb–Te–(Mo–W–U–Be–Co–Ni).

Known Ag-rich prospects associated with early Tertiary granites in the study region (table 1) are of two basic varieties: (1) vein/veinlet-dominated mineralization located outside of the parent granite body and (2) granite-hosted greisen deposits. The latter are large, bulk-tonnage deposits of near-economic potential (Kurtak and others, 1992); the former appear to be "distal" signals of deeper, and larger mineralized plutons. The best examples of polymetallic, Sn-bearing veins and sulfide replacements are present at the Ready Cash prospect (Hawley and Clark, 1974): lower-grade Sn–Ag mineralization associated with tourmaline breccias at Lookout Mountain probably has a similar origin. The ore mineralogy includes cassiterite and stannite, major arsenopyrite, sphalerite, galena, pyrite, and chalcopyrite, and minor wolframite, stibnite, bismuthinite, and argentite. The geochemical expression is Ag–As–Sn–Zn–Cu–Pb–Bi–W–Rb–B–Be–F–Li–Ga.

Tin greisen deposits are known in upper Ohio Creek in the A-6 quadrangle, and just south of the A-6 in upper Coal Creek. The Coal Creek deposit has been extensively diamond drilled and contains identified Sn–Ag–Zn resources. The Ohio Creek prospect lies within Denali National Park and has not been drilled, but has been extensively sampled (Warner and Dahlin, 1989). The ore minerals at both deposits include cassiterite and stannite, major arsenopyrite, sphalerite, pyrite, and chalcopyrite, and minor wolframite, galena, stibnite, bismuthinite, and argentite. Arsenopyrite and stannite–sphalerite geothermometry for the Coal Creek deposit indicate high (>400°C) temperatures of formation (Parker, 1991). Quartz, fluorite, topaz, and Li-rich white mica are common accessories; tourmaline is variably present. Minor Zn–Pb–Ag skarn is present in rare calcareous rocks near the Coal Creek prospects. The geochemical expression is Ag–Pb–Sn–Zn–Cu–As–Bi–W–Rb–B–Be–F–Li–Ga.

The Copper King and Nimbus prospects (table 1) appear to be slight variations on the major deposit types present in the study area. Both are distinguished by containing porphyry-textured felsic intrusive rocks with some stockwork quartz veining. At the Copper King prospect the majority of mineralization occurs in hornfels and rare skarn (developed from unit TRvs) as high-grade chalcopyrite–pyrrhotite–bornite masses. The high Cu and low As contents of this deposit (Hawley and Clark, 1974; Gage and others, 1998) also distinguish it from the other Au-bearing skarns in the region. Based on its metallogeny and associations, it is better classified as a Au-rich copper skarn (Newberry and others, 1997) and consequently the associated altered, Cu-bearing granite porphyry intrusion as a porphyry copper prospect. Variations in interpreted $^{40}Ar/^{39}Ar$ dates from this prospect (table 2, fig. 7) indicate thermal resetting by younger intrusions, and there may be multiple mineralization events present.

The Nimbus prospect, north of the Healy A-6 Quadrangle, lies within Denali National Park and has not been well studied. Swainbank and others (1977) describe it as a porphyry copper prospect, but molybdenite is more obviously abundant than any copper minerals and Mo is present in more anomalous abundance than is Cu (Gage and others, 1998). Mineralization is confined to altered, felsic porphyry dikes, which locally constitute a dike swarm (Swainbank and others, 1977). The exposed rocks associated with mineralization are too weathered and altered for reliable chemical analyses or dating and the nearby, less-altered dikes display ambiguous compositional characteristics. Some of these dikes possess compositions similar to demonstrably Cretaceous granites, others to demonstrably early Tertiary granites of the region. Dating of K-feldspar from a less-altered felsic dike yielded a plateau age of 61 Ma—intermediate in age between the two major types. Most likely this intermediate age indicates the presence of both Late Cretaceous and early Tertiary igneous activity. Due to the elevated Mo and Ag concentrations of the known mineralization (Gage and others, 1998), we categorize the bulk of hydrothermal activity as distally (?) related to a porphyry Mo system.

COMPOSITIONAL CHARACTERISTICS OF MAJOR IGNEOUS UNITS

All of the exposed volcanic rocks in the study area have experienced at least modest degrees of metamorphism, and although original textural features are sometimes preserved, the rocks are best described as 'metavolcanic'. Neither zeolites, prehnite, nor pumpellyite have been observed in these rocks and the minerals actinolite, chlorite, epidote, and calcite are nearly ubiquitous. Plagioclase is invariably altered to albite and original clinopyroxene grains are variably altered to fine-grained actinolite-bearing assemblages. The metamorphic mineralogy and lack of complete destruction of original igneous minerals indicates these rocks have experienced mid-greenschist facies metamorphism. The timing and number of metamorphic events experienced, however, is not presently interpretable.

Metamorphosed volcanic rocks rarely contain fossils and radiometric methods typically fail to penetrate through the metamorphism. Metavolcanic rocks are also notoriously variable in appearance and commonly display as much intra-unit as inter-unit variation in physical appear-

ance. Consequently, reliable identification and correlation of such rocks necessarily requires characteristics that transcend variability in volcanic and metamorphic conditions. The chemical compositions of such rocks, especially with regard to relatively immobile (insoluble) elements have been documented as particularly valuable in such identification and correlation (Pearce and Cann, 1973; Winchester and Floyd, 1977). Because the metavolcanic rocks of the map area have been previously identified and correlated based exclusively on hand-specimen appearance, and because there is considerable disagreement in the literature concerning the age, nature, and correlation of these rocks, we used compositional data to help make unit distinctions and correlations. We present this data here to clarify the origins and characteristics of the igneous rocks of the map area.

Most of the metavolcanic and many of the intrusive rocks of the map area are too altered for reliable categorization by standard major oxide compositional discriminants such as silica versus alkali diagrams. Gross compositions are better illustrated using 'immobile' element diagrams such as anhydrous normalized SiO_2 versus Zr/Ti (fig. 8). On such diagrams, the Paleozoic metavolcanic rocks ('D', 'bp', 'd', and 'ut', fig. 8A) display a compositional range from subalkali basalt to rhyodacite/dacite, the 'average' composition of Devonian metavolcanic rocks within the andesite field and the average for upper Paleozoic tuff in dacite/rhyodacite. Red colored clastic rocks, previously described as 'redbeds' (Jones and others, 1980) display a compositional range from basalt to dacite with most analyses of andesitic composition ('r', fig. 8A). Late Triassic metavolcanic rocks, herein correlated with the Late Triassic 'Wrangellia' flood basalts, in contrast, yields strictly basaltic compositions ('N', fig. 8A).

In contrast, intrusive rocks of the study area comprise two generally distinguishable groups (fig. 8b): older (Late Cretaceous) rocks of intermediate to felsic compositions ('k', fig. 8b) and early Tertiary rocks characterized by bimodal felsic and mafic compositions ('t' and 'T', respectively, fig. 8b).

That metamorphosed rocks possess elemental characteristics compatible with an igneous origin does not prove they *are* of igneous origin. The most controversial metamorphic rocks of the study area are the so-called 'redbeds', which possess a generally red color and characteristically clastic textures, but lack definitive evidence for sedimentary origins, such as fossils or sedimentary structures. Thin-section examination shows these rocks contain little quartz; major oxide chemical analyses (fig. 9A) show that they possess SiO_2 contents well below that of sandstone (even graywacke) but compatible with intermediate–mafic igneous rocks, as previously described (fig. 8A). Other compositional criteria, used both to identify sandstones and to identify their tectonic environments (fig. 9B) show that the red clastic rocks of the map area in general do not overlap compositionally with *any* sandstones of any tectonic setting, but again overlap compositionally with intermediate-mafic igneous rocks. It is hard to avoid the conclusion that, for the most part, these variably clastic red-colored rocks are primarily not continental sandstones.

A final means to compare the basaltic members of the different units is in terms of their relative Ti, Zr, and Y concentrations (fig. 10), which can also be used to infer tectonic environment of formation. Notably, Late Triassic volcanic rocks inferred to be stratigraphically equivalent to the Nikolai basalt of Wrangellia display immobile element ratios consistent with a 'within-plate' setting, compatible with the rift or mantle plume setting for Nikolai inferred by other workers (Barker and others, 1989; Richards and others, 1991; Plafker and Berg, 1994). Similarly, the early Tertiary mafic rocks ('T', fig. 10B) display 'within-plate' character, compatible with the bimodal (felsic + mafic) compositions (fig. 8B) of these rocks, a characteristic of extensional-related igneous systems.

Compositional comparisons between metavolcanic rocks of the study area and potential stratigraphic equivalents outside of the region (fig. 11) shows that some age-similar units are potential matches and others are not. The Triassic (Ladinian–Carnian) basaltic rocks of 'Stikinia', west-central Yukon, are sufficiently close in time to the Late Triassic (Norian) volcanic rocks of the study area to invite correlation. As shown by figure 11A, however, the strong contrast in immobile trace element contents of the two units rules out such a correlation. In contrast, immobile trace element compositions of Late Triassic Wrangellia basalts fall within the compositional range of the age-equivalent rocks in the study area, indicating a correlation is permissible. Similarly, the compositional similarities between late Paleozoic to early Triassic Skolai volcanic rocks and those of the early Triassic (and older?) red volcanic/volcaniclastic rocks of the study area invite a correlation between the two.

The Late Cretaceous and early Tertiary igneous rocks of the study area are primarily of intrusive character and consequently more easily distinguished based on hand-specimen characteristics. For example, Hawley and Clark (1974) suggested that the older (now known to be Late Cretaceous) intrusions were generally less felsic and the younger (now known to be early Tertiary) intrusions were more felsic. Such an assertion is demonstrated by figure 8B, based in part on immobile element ratios, but also by compositional classification employing normative major oxide compositions (fig. 12A). Although some strongly altered Cretaceous rocks (denoted by 'k') fall outside the general compositional fields, the bulk of analyses display a unimodal variation from quartz diorite and monzodiorite to syeno-granite, suggesting a fractionation-related assemblage. The normative quartz contents vary from 0 to greater than 20 percent, and on the whole increase with increasing normative orthoclase/anorthite ratio, again suggesting

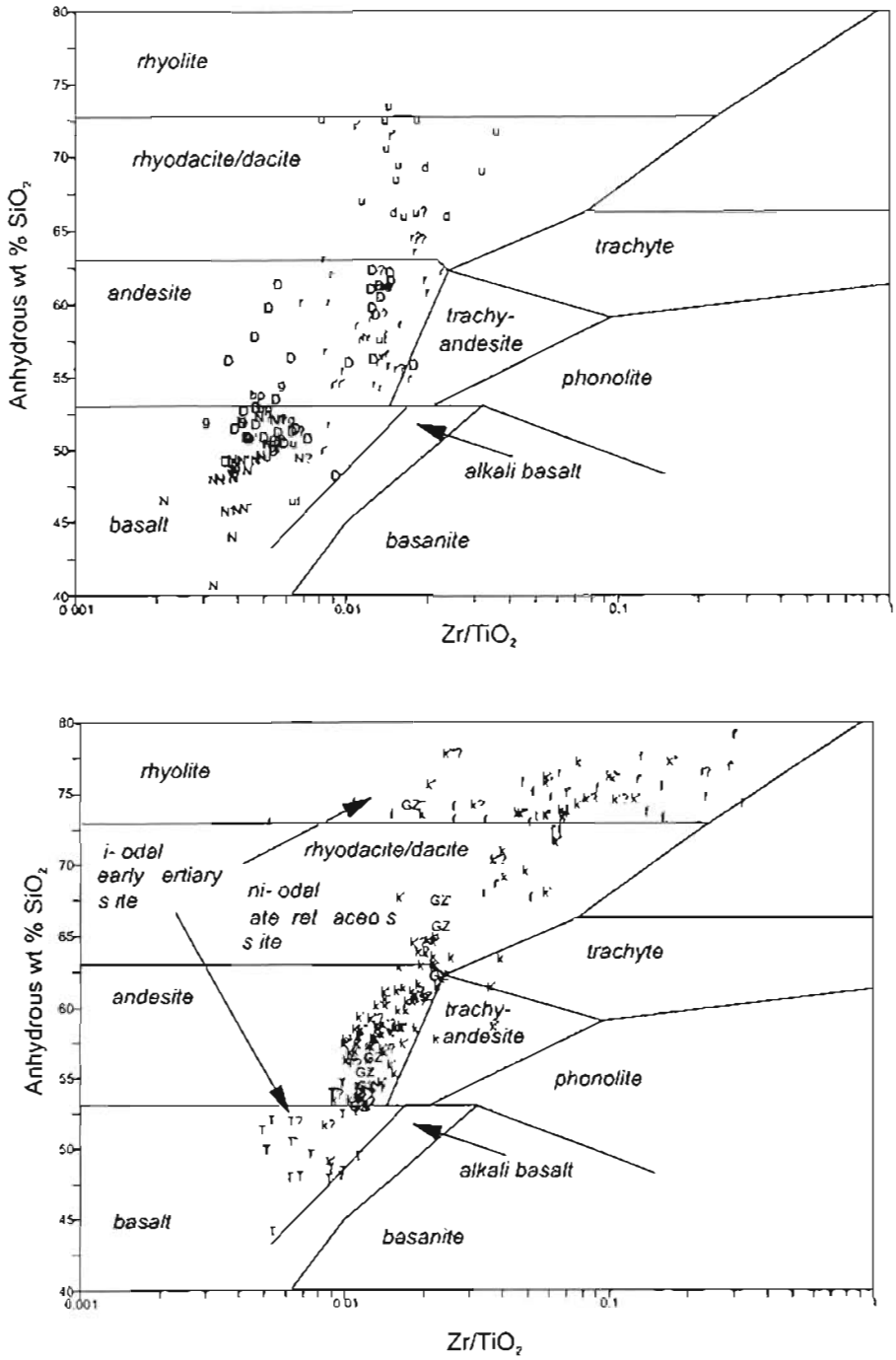

Figure 8. *Rock type classification for Chulitna area igneous and meta-igneous rocks employing the Zr/TiO_2 vs. SiO_2 discrimination diagram of Winchester and Floyd (1977). Symbol modifiers: ' = mineralogy indicates chemical alteration; " = highly altered; ? = rock type/age assignment based on rock composition—field evidence is ambiguous. Figure 8A: Paleozoic and Triassic meta-igneous rocks. D=andesite (unit Dv); r = red-colored volcanics (unit TRvs); u = tuff (unit uPzt); N = igneous rocks from units TRlb and Trb; n = late Triassic Nikolai basalt from the Wrangell Mountains; b = tuff in Paleozoic rocks of Broad Pass (Pzst). Figure 8B: Late Cretaceous and early Tertiary intrusive rocks: k = Cretaceous mafic–intermediate composition rock; GZ = plutonic rock from the Golden Zone deposit; k* = Cretaceous felsic composition rock; T = Tertiary mafic dike, f = Tertiary felsic intrusion. Data from Hawley and Clark (1974), Davis and Plafker (1985), Balen (1990), Barker and others (1994), Newberry and Solie (1995), and Gage and others (1998).*

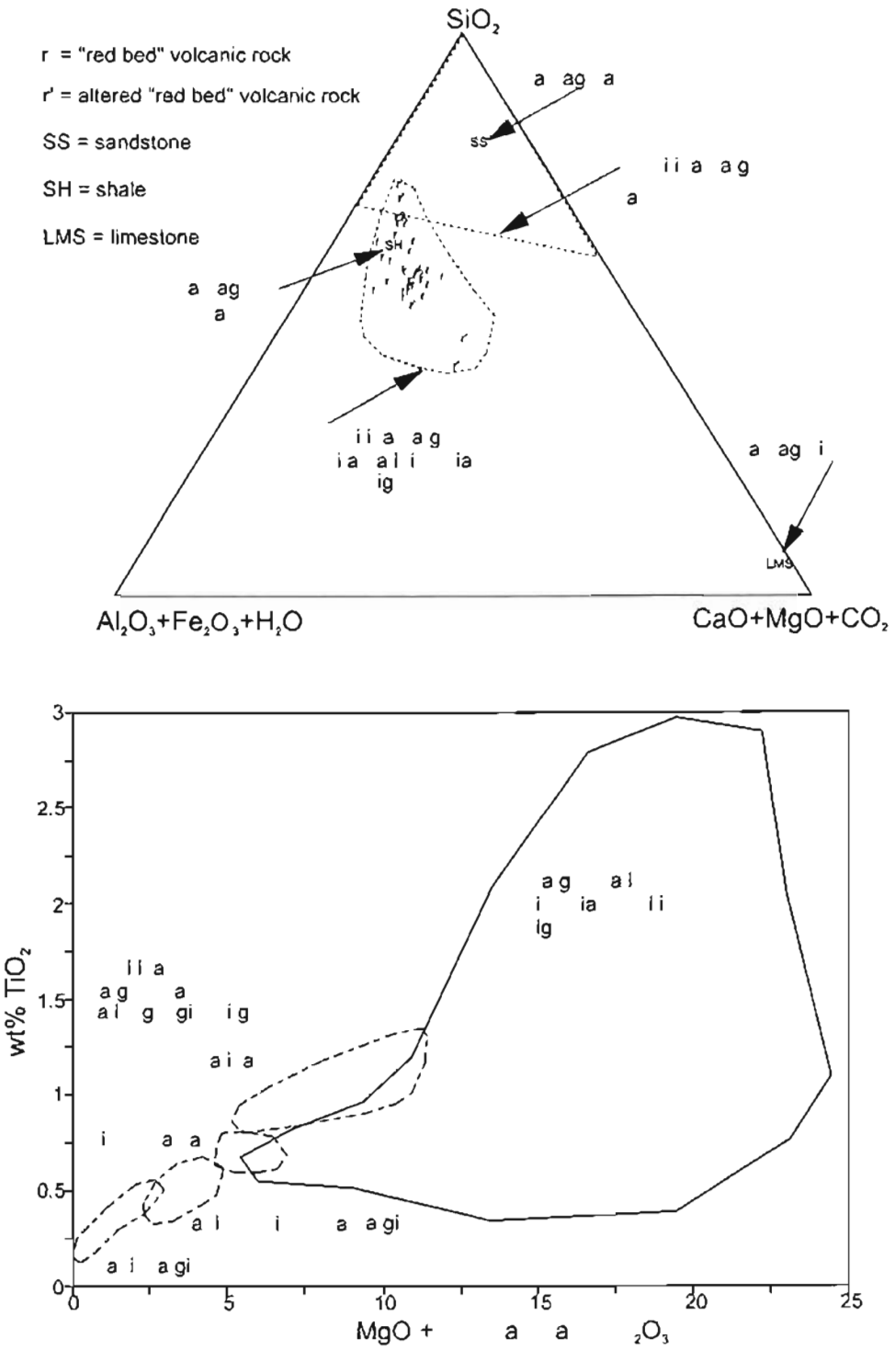

Figure 9. *Major element compositions of red clastic rocks ('redbeds') of the study area compared to those for sandstones and mafic–intermediate composition igneous rocks. Figure. 9A. Major element ratio diagram, modified from Mason (1966), showing that red clastic rocks of the study area do not compositionally resemble sandstones, but do resemble mafic–intermediate composition igneous rocks (and some shales). Figure. 9B. Major element-based tectonic classification scheme for sandstones (from Bhatia, 1983) showing compositions of clastic red rocks from the study area and range for typical mafic–intermediate composition igneous rocks.*

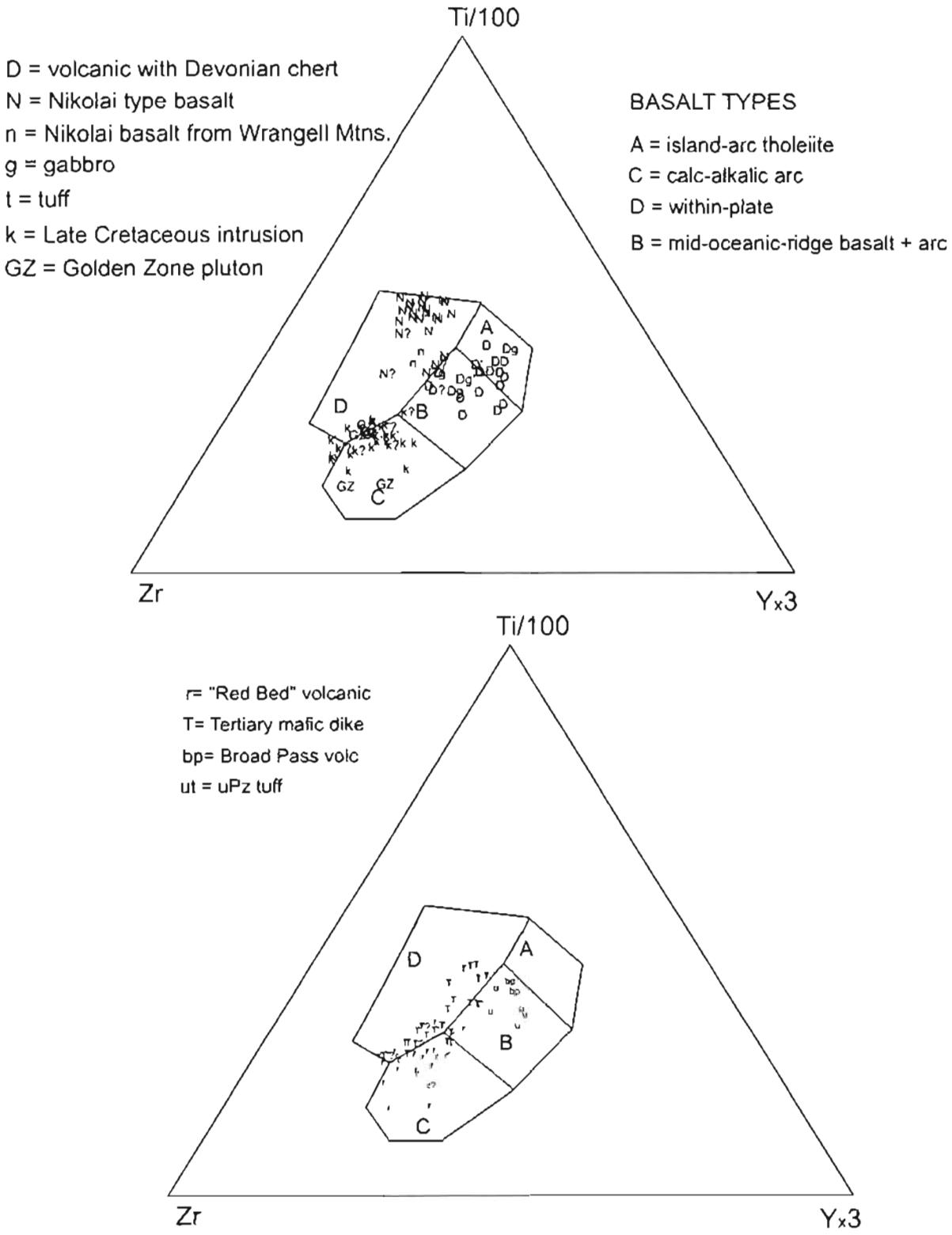

Figure 10. *Tectonic classification of Chulitna area mafic-composition igneous and meta-igneous rocks employing the Ti-Zr-Y discrimination diagram of Pearce and Cann (1973). Figure 11A: Mafic rock compositions from units TRlb, Trb, Dv, and Km. Figure 11B: Mafic rock compositions from units Tb, uPzt, uPzst, and TRvs. Symbols and data references as in figure 8.*

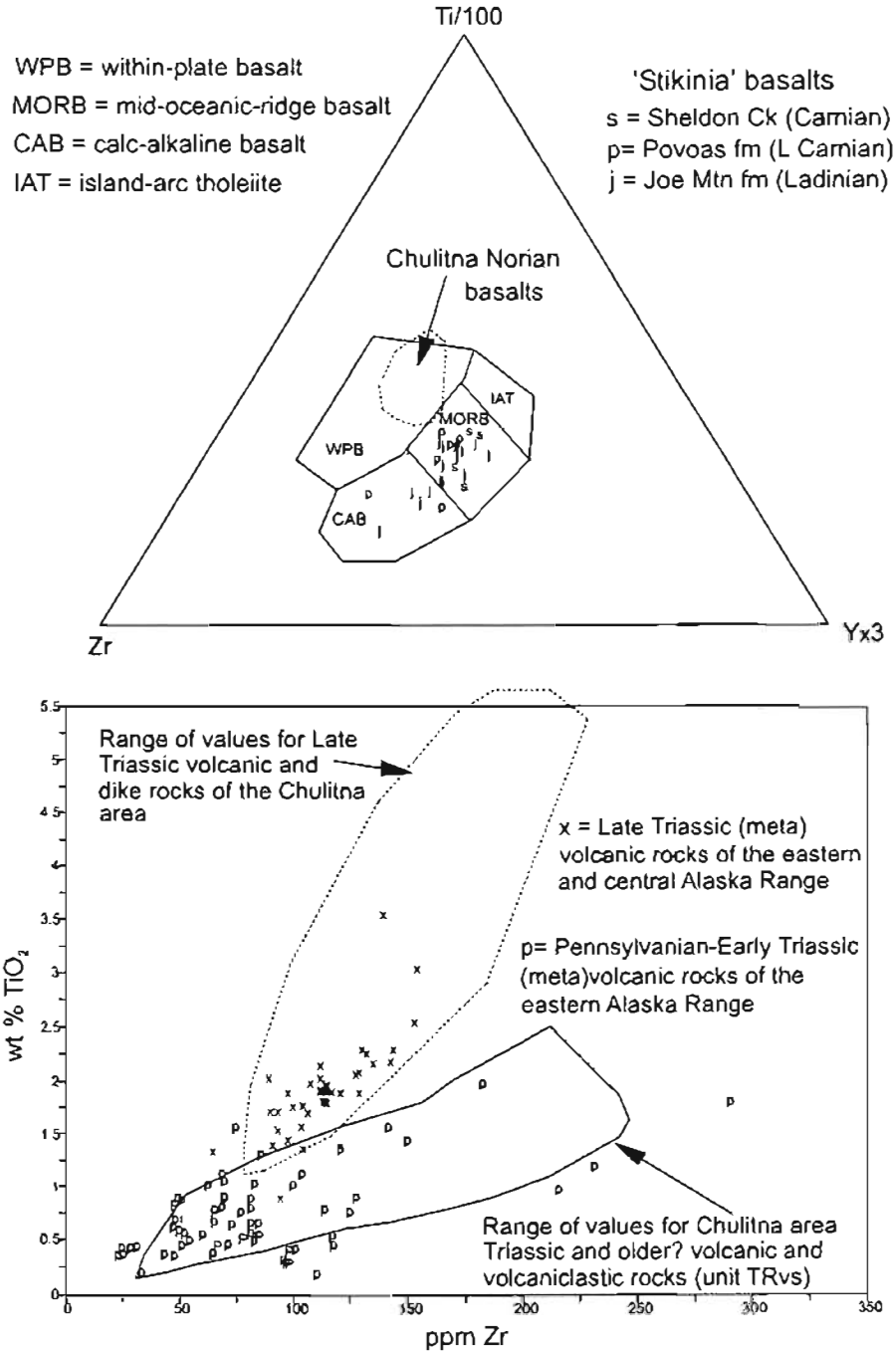

Figure 11. *Immobile element comparisons between late Paleozoic and Triassic metavolcanic rocks of the study area and potentially equivalent units from southern Alaska and eastern Yukon Territory. Data from Beard and Barker (1989), Barker and others (1994), Hart (1997), Athey (1999), and Gage and others (1998). Figure 11A. Y-Zr-Ti ternary diagram showing contrast between Triassic basalts of the 'Stikinia' terrane, Yukon Territory, and those of the study area. Although broadly similar in age (Landinian–Carnian vs. Norian) the compositional differences indicate that the Stikinia basalts are <u>not</u> equivalent to the 'within-plate' basalts of the study area. Figure 11B. Zr-Ti plot showing similarity in compositions of (1) Skolai arc volcanic/volcaniclastic rocks of southern Alaska with Early Triassic volcanic/volcaniclastic rocks of the study area, and (2) Late Triassic 'Wrangellia' flood basalt of southern Alaska and Late Triassic basalt of the study area.*

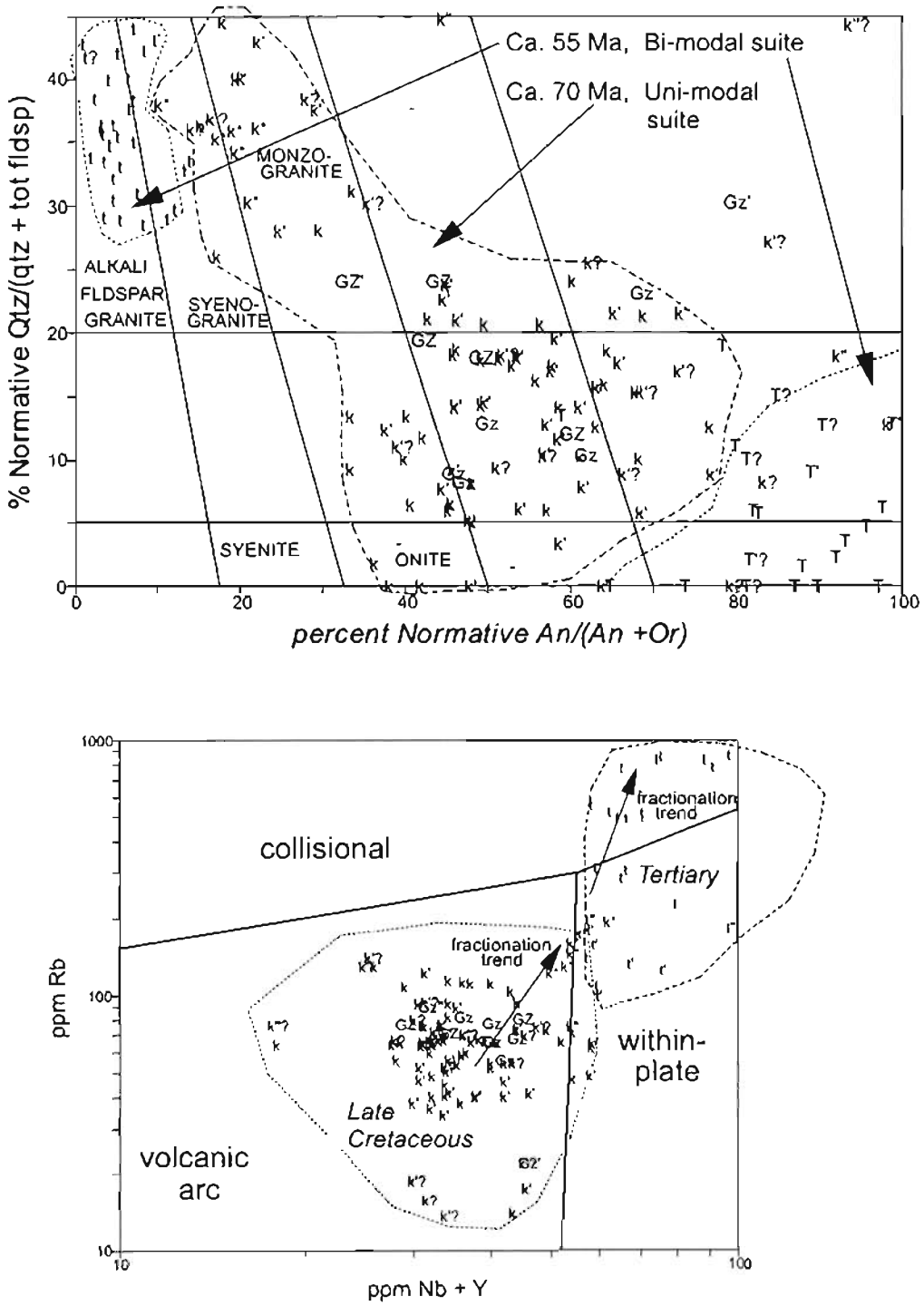

Figure 12. *Compositional characteristics of Late Cretaceous and early Tertiary intrusive rocks of the study area. Symbols: k = Late Cretaceous mafic–intermediate rock, k* = Late Cretaceous felsic rock; t = early Tertiary felsic rock, T = early Tertiary mafic rock, ' = chemically altered, " = very altered, ? = age assignment based on rock composition—field relationships are ambiguous. Data from Hawley and Clark (1974), Warner and Dahlin (1989), Balen (1990), Parker (1991), Gage and others (1998), and this study. Figure 12A. Normative rock type classification diagram, after Streckeisen and LeMaitre (1979). Figure 12B. Rb, Nb and Y data from Chulitna area Cretaceous and Tertiary intrusive rocks plotted on the granitoid tectonic setting diagram of Pearce and others (1984).*

a coherent fractionation assemblage. In contrast, the early Tertiary igneous rocks display strikingly bimodal compositions, dominated by basalt/gabbro + alkali–feldspar granite and lesser syeno-granite.

Minor element compositions of the intrusive rocks confirm differences in geologic setting accompanying the major element differences. A conventional means of identifying differences in tectonic environment of formation is through Rb vs. Nb+Y (fig. 12B), which cannot be employed for the metavolcanic rocks because Rb is highly mobile during metamorphism. The unmetamorphosed and generally weakly altered Late Cretaceous and early Tertiary rocks, however, define two compositional fields with little overlap (fig. 12B). The older intrusive rocks display a 'volcanic arc' signature whereas the younger intrusions display 'within plate' or 'collisional' signatures. Because Rb is known to increase with fractionation (Pearce and others, 1984) as shown by the arrows on figure 12B, the lower-Rb members of each suite are better indicators of the tectonic environment, thus, a 'within-plate' setting is more likely for the early Tertiary felsic rocks. This interpretation matches the trace element signature of the mafic early Tertiary rocks. Such a bimodal suite is conventionally explained by intrusion of basaltic magma into the lower crust, the anomalous heat causing partial melting and formation of the felsic melts.

Based on these compositional characteristics, we suggest the following changes in stratigraphic and tectonic interpretations for the metavolcanic rocks of the Chulitna region.

1. While we recognize some sedimentary rocks within the Chulitna region, much of what was previously mapped as 'redbeds' (oxidized, continental, warm-climate sandstone) is better described as a red volcanic wacke that compositionally resembles calc–alkaline arc volcanic rock. We have created two units from the 'Late Triassic continental redbeds' of Jones and others: (a) an older, largely volcaniclastic and volcanic portion that may extend into the Permian, but is at least as old as lower Triassic and (b) a younger, Late Triassic, commonly white quartz conglomerate that may interfinger with a fossiliferous, near-shore, marine calc–sandstone. Both members broadly resemble the upper Paleozoic to lower Triassic marine sedimentary and andesitic volcanic unit observed below the Nikolai basalt in the so-called 'Tangle subterrane' of Nokleberg and others (1994).
2. Trace-element chemistry of Triassic basalt in the Chulitna region correlates with that of extensional Late Triassic Nikolai greenstone mapped throughout southern Alaska and contrasts strongly with Stikinia terrane rocks of similar age. Consequently, the limestone–basalt unit in the Chulitna region is best described as a variant of the Wrangellia Nikolai basalt.
3. Volcanic rocks spatially associated with Late Devonian chert and—locally—with serpentinite fault slivers (our unit Dv) have the chemical characteristics of volcanic arc-related igneous rocks and are neither mafic/ultramafic dominated nor possess MORB-like compositions. We thus reject the suggestions of Jones and others (1981) that this sequence is an ophiolite and that it is a unique rock package in southcentral Alaska.
4. Devonian volcanics (our unit Dv) and tuffs (our units uPzt, uPzst) in the previously mapped West Fork and Broad Pass terranes (Jones and others, 1981) may be the same time–stratigraphic unit.
5. In summary, our evidence contradicts the assertion that Chulitna is a 'unique terrane' (Jones and others, 1981), but is compatible with the hypothesis that it represents a variant of the Wrangellia terrane of eastern Alaska. We believe it comprises a composite of Chulitna, West Fork, and Broad Pass terranes (Jones and others, 1981) of earlier usage.

DESCRIPTION OF MAP UNITS

BEDROCK UNITS

SEDIMENTARY AND VOLCANIC ROCKS

Tertiary deposits

Ts **Gravel and sand** (Miocene? to Paleocene?) — Orange- to buff-colored, well-sorted, clast-supported, sandy pebble–cobble gravel and sand (sheet 1, photo 3). Measured thicknesses of this unit range from 6 to 45 m. The deposit shows varying degrees of orange and purple-black (manganese oxide) discoloration and weathers to light buff or grayish brown. While typically poorly to moderately consolidated, the unit is locally indurated enough to approach a true conglomerate. The deposit forms bare, near-vertical cliffs where incised by streams and is prone to gullying. Clasts are sub-rounded to very well rounded, and median clast size is approximately 5 cm in diameter. The largest cobbles are generally not more than about 15–20 cm diameter, although can locally exceed 40 cm diameter. Clast lithology is typical of an Alaska Range source area, including chert, argillite, graywacke, volcanic rocks, felsic to intermediate intrusive rocks, and the distinctive conglomerate

from the Cantwell Formation (Capps, 1940) with well-rounded clasts of quartz, gray to black chert, sandstone, and argillite. Many of the granitic to dioritic clasts are highly weathered, especially the more mafic ones. The deposit is predominantly massive to thick-bedded, and has an overall horizontal fabric. It is locally very well bedded with crosscutting channels and crossbedding, especially in sand beds and in some pebble beds. Local channeling is most apparent in sandy units. Sand beds typically constitute no more than 2–5 percent of the section, but are locally much more abundant. Sands occur mostly as broad lenses with an average thickness between 10 and 20 cm and a maximum measured thickness of 80 cm. Silt bodies are very rare, occurring as lenses up to 35 cm thick that may locally exhibit soft-sediment deformation structures due to loading. Pollen samples collected from the rare silt beds were too oxidized to be analyzed. The upper contact of the deposit is erosional, forming a slightly irregular surface that appears to dip to the south. This deposit is fluvial in origin, and was laid down by a very active, sediment-laden stream system that probably developed in association with the uplift of the Alaska Range during Tertiary time. This deposit is probably correlative with the Nenana Gravel on the north side of the Alaska Range. This unit is preserved in the down-dropped, fault-bounded block, or graben in Broad Pass in the southeastern portion of the map, where it can be observed in exposures up to 100 m thick.

Tcs **Coal-bearing sandstone** (Oligocene?) — Poorly to moderately consolidated, light gray to yellow pebbly sandstone and pebble conglomerate with smaller quantities of brown micaceous silty claystone, carbonaceous claystone, and lignite. Lignite seams are dark brown on both fresh and weathered surfaces and break with a shaly fracture or irregularly along shrinkage cracks. Seams dip less than 10 degrees; are 5 to 10 ft thick and contain 0.2 to 0.4 percent sulfur and 10 to 20 percent ash with a heating value of 5,500 to 7,100 Btu/lb (Hopkins, 1951; Merritt and Hawley, 1986). Thought to be correlative with Oligocene coal-bearing deposits at the Dunkle coal mine on Camp Creek, about ten miles to the west (Csejtey and others, 1992).

Kahiltna Assemblage

The Kahiltna assemblage (Reed and Nelson, 1980, Csejtey and others, 1978, 1982, 1992; Nokleberg and others, 1994) is found in the northwest and eastern map areas, and may underlie the intervening older rocks, although a recent study suggests that Kahiltna-age rocks were deposited into two separate basins on either side of the Chulitna area, which formed a syndepositional structural barrier (Eastham and others, 2000). The Kahiltna assemblage consists of a monotonous, highly deformed flysch succession of fine-grained lithic sandstone, argillite, highly siliceous argillite, and rare conglomerate and limestone of prehnite–pumpellyite metamorphic grade. This predominantly turbidite assemblage is several thousand meters thick. In the eastern map area, bedding and cleavage typically dip to the southeast, and fold vergence is predominantly to the northwest. In the northwest, typical bedding and cleavage dip is to the northwest with fold vergence predominantly to the southeast. Regionally the Kahiltna assemblage underlies a large area of southcentral Alaska, and locally includes large thrust sheets or nappes of Upper Triassic pillow basalt (Jones and others, 1980). Age of these rocks is based on Early Cretaceous fossils (belemnite guards and *Inoceramus* prisms) similar to those reported by Jones and others (1980) recovered from the northwest map area (loc. 2–4 in Blodgett and Clautice, 2000) as well as regionally reported *Inoceramus*, belemnites, and *Buchia sublaevis* of Cretaceous age, and radiolarians of Upper Jurassic age (Jones and others, 1980).

Below we subdivide the Kahiltna assemblage into three mappable lithologic units: (1) argillite and sandstone, (2) sandstone and argillite and (3) conglomerate.

KJas **Argillite and sandstone** (Upper Jurassic to Lower Cretaceous) — Dark gray to very dark gray and black argillite (locally phyllitic) and dark gray sandstone. Rocks weather brown, orange-brown, and reddish-orange. Argillite is greater than 50 percent of this unit and locally sandstone may be as little as 10 percent of the unit. Cleavage is prominent in this unit and is commonly the dominant outcrop characteristic. Cleavage is commonly parallel to bedding, however, where it is not, the relationship generally indicates folding or overturning with a northwest vergence. North of the East Fork Chulitna River this unit is locally cross-cut by mafic and felsic dikes. White quartz veining, locally with sulfides, and locally as crystal-filled vugs and fractures, is up to 30 cm thick and locally up to 2 m thick.

KJsa **Sandstone and argillite** (Upper Jurassic to Lower Cretaceous) — Sandstone with much lesser argillite. Predominantly dark gray, poorly sorted, sub-angular, fine- to medium-grained lithic sandstone, rhythmically layered with dark gray, locally carbonaceous argillite. Sandstone weathers dark gray, medium gray, and locally light gray or orange brown. Sandstone forms about 80 percent of this unit. Sandstone beds are laterally continuous, have sharp, non-erosive bases, are generally thin-bedded with lesser medium-bedded, and form rare amalgamated beds to 50 cm thick. Beds are massive or graded, with Bouma intervals T_{a-e}, T_{bde}, and T_{de}

common. The depositional environment for this unit is a middle submarine fan (Mutti and Ricci Lucchi, 1978) on the basis of sedimentary structures and bedding characteristics. Sandstone locally contains carbonate along with the ubiquitous clay matrix, and framework clast estimates are 70 percent quartz, 20 percent black argillite (low-grade metamorphic rock) including riprap clasts, 10 percent gray chert (with rare white tripolitic chert), and minor white mica. Cleavage is the dominant structural feature. Andalusite-spotted hornfels is locally found adjacent to plutons and dikes. In the headwaters of Antimony Creek it is cross-cut by a gabbro dike of probable Tertiary age. Includes rare conglomerate that is shown as map unit KJc where thicker than 1 m.

KJc **Conglomerate** (Upper Jurassic to Lower Cretaceous) — Medium gray, poorly sorted, matrix-supported, polymictic pebble to cobble conglomerate. Matrix is fine- to medium-grained sandstone and constitutes about 15 to 20 percent of the rock. Clast estimates from the eastern part of the map area are 70 percent quartz, 20 percent black argillite, and 10 percent gray chert (with rare white tripolitic chert). Cobble to boulder conglomerate is noted to the northwest with sandstone argillite, siltstone, and conglomerate clasts and minor coarse sand sequences with a–b Bouma cycles.

Older Assemblage

The older assemblage forms the core of the map area and may lie in thrust contact above younger Kahiltna assemblage rocks. We believe it comprises a composite of Chulitna, West Fork, and Broad Pass terranes (Jones and others, 1981) of earlier usage. This linkage is based on geophysical and lithochemical similiarities between Devonian volcanics (unit Dv) and associated serpentinite within the classic Chulitna terrane and serpentinite and volcanics (within units uPzt, uPzst, and uPzs) of both West Fork and Broad Pass terrane. All units within this assemblage have been subjected to low-grade regional metamorphism; pre-Jurassic units have experienced greenschist-facies metamorphism.

KJs **Calcareous sandstone and argillite, with coquinoid limestone** (Upper Jurassic to Lower Cretaceous) — Predominantly medium gray, poorly and very poorly sorted, sub-angular with lesser sub-rounded, fine- to medium-grained, tan to light gray, orange-brown weathering, calcareous, lithic sandstone. The sandstone is interlayered with dark gray argillite, and rare coquina limestone to 2 m thick composed of comminuted *Buchia sublaevis* shells (Valanginian, Lower Cretaceous age, loc. 11, 13, 38, 39, 93 in Blodgett and Clautice, 2000). Rare, thin-bedded, quartz grain-bearing carbonate (rubble only). Calcareous sandstone is the distinguishing lithology of this unit and composes less than 25 percent, whereas the unremarkable argillite constitutes more than 70 percent of this unit. Sandstone bedding is thin, parallel, laterally continuous, and conformable with coquina beds where the bounding clastic rocks are very-fine-grained red- to maroon-weathering sandstone and siltstone. The distinctive coquinoid limestone weathers maroon to dark reddish-brown and is composed of broken shells, which locally range to 4 cm in diameter. Contact relationships of this unit (whether faulted or depositional) are uncertain. It is most prevalent in the northwest map area, apparently overlying and folded with basaltic tuff and limestone of unit TRlb, but is also present in the central map area, east of Copeland Creek, based on a *Buchia* occurrence (locality 93, Blodgett and Clautice, 2000) within calcareous sandstone and thin-bedded limestone. This unit is isoclinally folded, and the resulting cleavage is the dominant fabric in the hinge regions and less dominant distal from the hinges. The closely spaced cleavage is especially prominent in the argillaceous lithologies where it locally forms pencil cleavage.

Petrographic analyses indicate sandstone framework grain averages are 60 percent chert, 10–15 percent polycrystalline quartz, 10–20 percent monocrystalline quartz, 10 percent to minor sedimentary rock fragments, 5 percent to minor plagioclase, minor to trace volcanic rock fragments, and other trace minerals include white mica, hornblende, and glauconite. Aqua-blue chert clasts are rare but distinctive. Sandstone matrix is iron-rich carbonate and calcite, with only a minor clay component. Matrix ranges from 5–15 percent of the rock, with an average of less than 10 percent. Porosity in sandstone is very minor due to secondary carbonate cement. Sandstone petrography indicates a recycled orogenic provenance. Furthermore, the provenance is more characteristic of the collisional recycled orogenic provenance than the foreland uplift recycled orogenic provenance due to: (1) more abundant plagioclase relative to lithic rock fragments, and (2) more polycrystalline quartz relative to sedimentary rock fragments. The coquinoid limestone layers within this map unit are rare but significant, and similar to coquinoids of Valanginian age known in the Kandik basin of east-central Alaska and Yukon Territory. Additionally, they are similar to coquinoids on the Alaska North Slope, which crop out along the foothills of the Brooks Range from the DeLong Mountains in the west to the Shaviovik

front, east of the Dalton Highway. All of these deposits are within a siliciclastic stratigraphic package and represent shelfal deposition, in water depths of less than about 125 m. All of these thin (0.2–3.0 m) carbonate horizons may represent a local sediment flushing, winnowing, and shell disaggregation (with no substantial transport) due to episodic high-energy storms, or this stratigraphy records destructive reorganization of pelecypods which included some down-slope transport.

The relationship of this unit to Kahiltna rocks of similar age is unclear. It is possible that it represents a near-shore facies of the deeper-water Kahiltna assemblage.

Jac **Argillite, cherty argillite, and minor cherty tuff and basaltic tuff** (Middle? to Upper Jurassic) — Mostly argillite exhibiting complex deformational fabrics and sub-greenschist metamorphic mineralogy. This unit is characterized by argillite and cherty argillite, with minor cherty tuff and basaltic tuff. Light gray to black rhythmically bedded chert predominates. In places this unit is highly sheared and phyllitic. Radiolarians from this unit are of Late Jurassic (Callovian to Tithonian) age (loc. 106, 107, 111, 112 in Blodgett and Clautice, 2000), while a single locality (locality 5) was recognized to be of undifferentiated Jurassic age.

Js **Calcareous sandstone, sandy limestone, and argillite** (Lower Jurassic) — Thin to medium, regularly bedded, brown weathering calcareous sandstone, sandy limestone and argillite. In places phosphatic and fossiliferous. Ammonites within this unit are of Sinemurian, Early Jurassic age (loc. 104, 105, 132, 137, 147, 152 in Blodgett and Clautice, 2000).

TRrb **Redbed sandstone and conglomerate** (Upper Triassic) — Red- to maroon-weathering, calcareous siliciclastic rocks (especially sandstone, siltstone, and conglomerate; sheet 1, photo 5). The sandstones are commonly coarse-grained, hematitic, red-weathering, (but less commonly light-green weathering) with local calcareous cement. Red-weathering, matrix-supported, well-rounded pebble conglomerate with pebbles of white quartz, basalt, and volcaniclastics is a distinctive lithology of this unit. No fossils were found within this unit for stratigraphic control, but these rocks appear to overlie the Upper Triassic limestone and basalt unit (TRlb). In rubble-crop exposures, with a decrease in hematite content and an increase in sandstone maturity, calcareous cement, and thin limestone layers, the lower portion of this unit appears to grade into Upper Triassic unit TRs. It is uncertain whether this is truly a gradational contact, structural, or erosional contact.

TRs **Brown sandstone and argillite** (Upper Triassic) — Thick-bedded, yellow-brown weathering sandstone and argillite with minor calcareous sandstone and sandy limestone. Abundantly fossiliferous horizons yield large (4 cm diameter) heterastridium (sheet 1, photo 6), snails, and bivalves of Late Triassic, Norian to Rhaetian age (loc. 150, 151 in Blodgett and Clautice, 2000). Contact relations with adjacent units are not entirely certain. These rocks may represent a transitional, near-shore environment between the redbed sandstone and conglomerate (TRrb) above and the Upper Triassic limestone (uTRl) and limestone/basalt unit (TRlb) below.

TRlb **Basalt, basaltic tuff, and limestone** (Upper Triassic) — Predominantly massive (occasionally pillowed) basalt and basaltic tuff 50–100 m thick, interlayered with fine-grained gray limestone (sheet 1, photo 4). Near some contacts with basalt the limestone is coarsely recrystallized and sheared, other contacts display fossiliferous limestone immediately adjacent to basalt. Major to minor chlorite–albite–carbonate–hematite alteration in the basalt is ubiquitous. The basalt is subalkaline (fig. 8a) and tholeiitic, characterized by "within-plate" trace-element abundances (fig. 10), strongly magnetic, and dark-green weathering. Trace- and major-element concentrations in the basaltic rocks (figs. 8a, 10a) are indistinguishable from those of the Late Triassic Nikolai greenstone flood basalts (Davis and Plafker, 1985; Barker, 1994). The only other known Triassic basalts of significant thickness in the general area are in the 'Stikinia' terrane of the western Canadian cordillera; these have trace-element contents that contrast significantly (fig. 11) with those of the Chulitna area (Hart, 1997). The limestones contain colonial scleractinian corals, megalodontid bivalves, and the brachiopod *Spondylospira lewesensis* (Lees), and the age is Norian. Slightly younger, Norian to Rhaetian faunal assemblages are found in a light brown, calcareous sandstone within unit TRs, which lies unconformably(?) above TRlb. Below and intruded by basaltic dikes of this unit is unit Trvs, of red-colored volcaniclastics and sandstones. Preliminary paleomagnetic investigations (Stone and others, 1999) indicate a paleolatitude of formation for TRlb basalt at 5 degrees, consistent with the paleontologic record and the paleolatitude of the Nikolai flood basalt of southern Alaska. It is not known whether these rocks were normally or reversely magnetized, therefore it is not known whether this represents a paleolatitude north or south of the equator. Although faunal assemblages in TRlb limestones are slightly younger (Norian) than those associated with the limestones above the Nikolai basalt (Carnian), the basalts are compositionally indistinguishable from Nikolai greenstone. Given the similar chemistry and that preliminary paleomagnetic data suggest a similar latitude of formation, we infer that

basaltic rocks within TRlb constitute a slightly younger variant of the Nikolai units of southern Alaska, perhaps a moving hot spot that is part of the Wrangellia terrane, and consequently that it—and by inference the associated rocks—is a part of the Wrangellia terrane as suggested by Jones and others (1980).

TRb **Basaltic dikes and sills** (Upper Triassic) — Fine-grained, equigranular to porphyritic, strongly magnetic, mafic intrusive rocks, similar in appearance and indistinguishable in composition from the basalt of unit TRlb. Has been noted most commonly as dikes and sills, 1–3 m wide, as well as plugs (?) or composite dikes in unit TRvs. $^{40}Ar/^{39}Ar$ dating indicates a minimum age of 179 Ma (table 2). These relations indicate that unit TRlb is younger than TRvs, contradicting the inferred stratigraphic relations of Jones and others (1980).

uTrl **Limestone** (Upper Triassic) — Thin- to thick-bedded limestone with subordinate shale and calcareous siltstone, well bedded. Unit at least 300 m where well exposed in the upper reaches of Long Creek. Carbonate lithologies include mudstone, wackestone, packstone and even rudstone (rare); locally with silty and argillaceous admixtures. A prominent interval composed of in-place colonial scleractinian thicket reefs crops out in the upper canyon of Long Creek. At this locality, the unit contains a rich and well-preserved Norian-age fauna of brachiopods, scleractinian corals, bivalves, and less common gastropods (loc. 51–53 in Blodgett and Clautice, 2000, Stanley and Yarnell, in press). To the south, the unit can be traced along strike for several miles within unit TRvs. Whether the contact is structural or depositional is uncertain (plate 1, photo 9).

TRvs **Red-colored tuff, andesite, basalt, graywacke, conglomerate** (Middle? to Lower? Triassic, possibly older) — A predominantly volcanic and volcaniclastic unit of red-colored lithic tuff, lithic conglomerate, graywacke, finely laminated tuffaceous siltstone and mudstone with minor basalt to dacite flows (sheet 1, photos 1, 7, and 9). Previously mapped as part of Jones and others' (1980) sedimentary redbeds, we delineate these primarily volcanic rocks (fig. 9) as a separate and older unit. Volcanic members are predominantly calc–alkalic andesite tuffs and tuff breccias, but compositions range from calc–alkaline basalt to dacite. Generally non-magnetic due to oxidation of primary Fe–Ti oxides to hematite; the combination of this oxidation and the common occurrence of calcite suggests conditions alternated between sub-aerial and subaqueous deposition. Coarser volcaniclastic members are often calcareous, with a predominantly medium- to very coarse-grained, poorly sorted matrix containing occasional feldspar, clinopyroxene, and hornblende crystals. Lithic clasts are subangular and consist of predominantly mafic volcanics frequently altered to chlorite, hematite, and calcite. Other lithic fragments include quartz, polycrystalline quartz, felsic volcanics, plutonic, and metamorphic rock.

Where present near Cretaceous intrusions, unit is hornfelsed to a green, hard rock with remnant tuffaceous textures. Unconformably underlain by limestone containing fossils with ages ranging from Pennsylvanian(?) to Permian (loc. 24, 25 in Blodgett and Clautice, 2000). The unit is locally cut by dikes and sills of tholeiitic basalt composition indistinguishable from unit TRlb, which further implies a pre-Upper Triassic age. The compositions (for example, fig. 11b) and lithologies (dominantly volcanic and volcaniclastic rocks) of the lower portion indicate a volcanic arc affinity. This unit is correlative with the late Paleozoic and Early Triassic sedimentary and andesitic tuff unit of the Tangle subterrane (Nokleberg and others, 1994).

This unit directly overlies Permian limestone; where the limestone is absent it overlies Pennsylvanian–Permian mudstone and graywacke. The basal contact of the unit is a red chert–pebble conglomerate; the chert contains upper Devonian radiolaria that are apparently derived from unit Dc.

Consequently, we infer that in places the lower contact of unit TRvs represents a local unconformity. The common red color of this unit is due to its andesitic–basaltic bulk composition and to syngenetic or diagenetic oxidation. Rarely, if ever, is this unit a hematitic sandstone, or a "redbed" in the commonly accepted use of the term. Total thickness is unknown, but at least 300 m thick and probably quite variable in thickness.

lTRl **Limestone** (Lower Triassic) — Thin-bedded, light gray, light brown weathering mudstone and packstone. Recognized within small, high-angle fault slivers in two localities in the northeastern map area. Both exposures are less than 4 m in strike length and 1–2 m thick. In the easternmost exposure, Nichols and Silberling (1979) recognized 13 identifiable species of ammonite fossils in a single 10-cm-thick bed. The collection is significant because the closest rocks of similar age (Smithian) and equatorial paleolatitude (10 degrees) are found in northern Washington. At the time of our visit this exposure was in a cat trail near the Golden Zone mill and all fossils had been "mined." The second locality, about 2 km to the west, is exposed as orange-brown weathered, silicified packstone to wackestone with poorly-preserved fossil material in rubbly outcrop over a few square meters above a trail along an old flume (loc. 23 in Blodgett and Clautice, 2000). This unit is only

exposed in high-angle fault slivers, for example, in fault contact with red-colored, coarse-grained volcaniclastics from unit TRvs.

Pl **Limestone** (Upper Permian) — Approximately 100 m thick succession of limestone subdivided into distinct lower and upper units (fig. 13). Lower unit composed primarily of medium- to thick-bedded, light to medium gray weathering limestone. Carbonate lithology is predominantly encrinoidal packstone to grainstone. Upper unit composed of medium- to thick-bedded limestone, light gray to orange-yellow weathering and locally highly silicified. Lithologies include mudstone, packstone and grainstone, frequently with argillaceous partings. Horridonid brachiopods are common near top of upper member. The limestone contains abundant megafauna of "Arctic Permian" type consisting of brachiopods, bryozoans, pelmatozoan debris, solitary rugose corals, ostracods, and trilobites of Late Permian age. Conformably and gradationally overlies a succession of Permian-age argillite and graywacke and is unconformably overlain by a thick "red bed" volcaniclastic sequence (unit TRvs).

PPs **Permian mudstone and graywacke** (Pennsylvanian? to Permian) — Unit is at least 200 m thick and composed of thinly bedded mudstone and graywacke (sheet 1, photo 2). Lower part of unit dominated by gray-green graywacke turbidites that weather to yellow-brown, composed of lithic sandstones, 3–60 cm thick, interbedded with thin intervals of mudstone. Fossils not observed in the lower part of the unit. Thin-bedded, medium to dark gray and yellow-brown mudstone and siltstone predominate in the upper part of this unit, with trace fossils of the ichnogenera *Chondrites* and *Scalarituba*, and relatively scarce small brachiopods, bivalves, and bryozoans near the top of the succession. Unit conformably and gradationally underlies Permian limestone unit (Pl). Unit is well exposed along north—south-trending ridge in SE1/4,NE1/4 Sec. 17, T20S, R11W, and along hillside both above and below ditch in NW1/4NE1/4 Sec. 4, T20S, R11W.

uPzt **Tuff** (upper Paleozoic?) — Described by Jones and others (1980) as unit JTRt, part of the West Fork terrane, this unit is characterized by predominantly dark gray-green, andesitic to rhyodacitic composition ash and crystal tuff, subordinate argillite, and cherty argillite, siltstone, and graywacke, and minor volcanic flows. The ash tuff is commonly "flinty" and layered in 5–30 cm varicolored beds of green, white, and tan, and is clearly welded in places (plate 1, photo 8). Wispy layering is common within beds. The coarser crystal-lithic tuff occurs in thicker beds (greater than 1 m), and hand specimens could be misidentified as sandstone. Basaltic- to andesitic-composition, angular, clast-supported tuff breccias occur in poorly-exposed lower-elevation sites. Such rocks are compositionally indistinguishable from the mafic volcaniclastic rocks of unit Dv (figs. 8a, 10). The interlayered sedimentary rocks are principally volcaniclastic sandstones, which appear to be reworked tuff from the same sequence. Compositional and textural similarities between this unit and unit Dv suggest that unit uPzt represents the upper (felsic tuff-dominant) portion of unit Dv, partly removed during Early Carboniferous erosion prior to deposition of unit PPs. Consequently, we infer that the "West Fork terrane" of Jones and others (1980) is indistinguishable from the Paleozoic rocks in the Chulitna region.

uPzst **Argillite and tuff** (upper Paleozoic?) — With lesser siltstone and chert. Compositions and character of the varying rock types are the same as uPzt, although the relative proportions are different. In this area, sedimentary rocks comprise about 85 percent of the unit, volcanic tuffs about 15 percent. The contact with uPzt is transitional, and placed where sedimentary rocks are more abundant than tuffaceous rocks. This unit may be equivalent to unit PPs, but definitive evidence is lacking.

uPzs **Chert, argillite, and graywacke** (upper Paleozoic?) — Part of Jones and others (1980) Broad Pass terrane and Csejety and others (1992) Cretaceous melange. This unit is poorly exposed, and includes a variety of lithologies found in steeply incised drainages where continuous traverses are not feasible. Lithologies encountered include bedded chert (upper Paleozoic based on radiolarians, Jones and others, 1980) and carbonaceous, fissile black argillite with yellow- and orange-weathering salts, basalt, cherty tuff, green volcaniclastic rock, siltstone, graywacke (with black and occasionally red chert grains) and clast-supported, white quartz–pebble, black argillite (occasionally red argillite) conglomerate. Limestone (unit Dl) crops out in Copeland Creek and Long Creek canyons and contains fossils thought to be identical to a Givetian (late Middle Devonian) fauna from Healy B-4 Quadrangle described by Blodgett (1977). A narrow, northeast-trending aeromagnetic high traverses the unit and in three locations coincides with outcrops of very magnetic serpentinite as found to the northwest associated with unit Dv. Based on similar lithologies, upper Paleozoic fossils, and the serpentinite trend, this "unit" may in part, represent a structural repetition of the upper Paleozoic rocks found to the northwest.

Dv **Andesitic tuff and flows** (Upper Devonian) — Predominantly green-weathering, pyroxene andesite tuff and flows, but compositions range from island-arc tholeiitic basalt (locally pillowed) to dacitic tuff (fig. 8a). Previously mapped as "Tertiary gabbro breccia" in the Golden Zone mine area (Hawley and Clark, 1974) and

Upper Permian Limestone Section

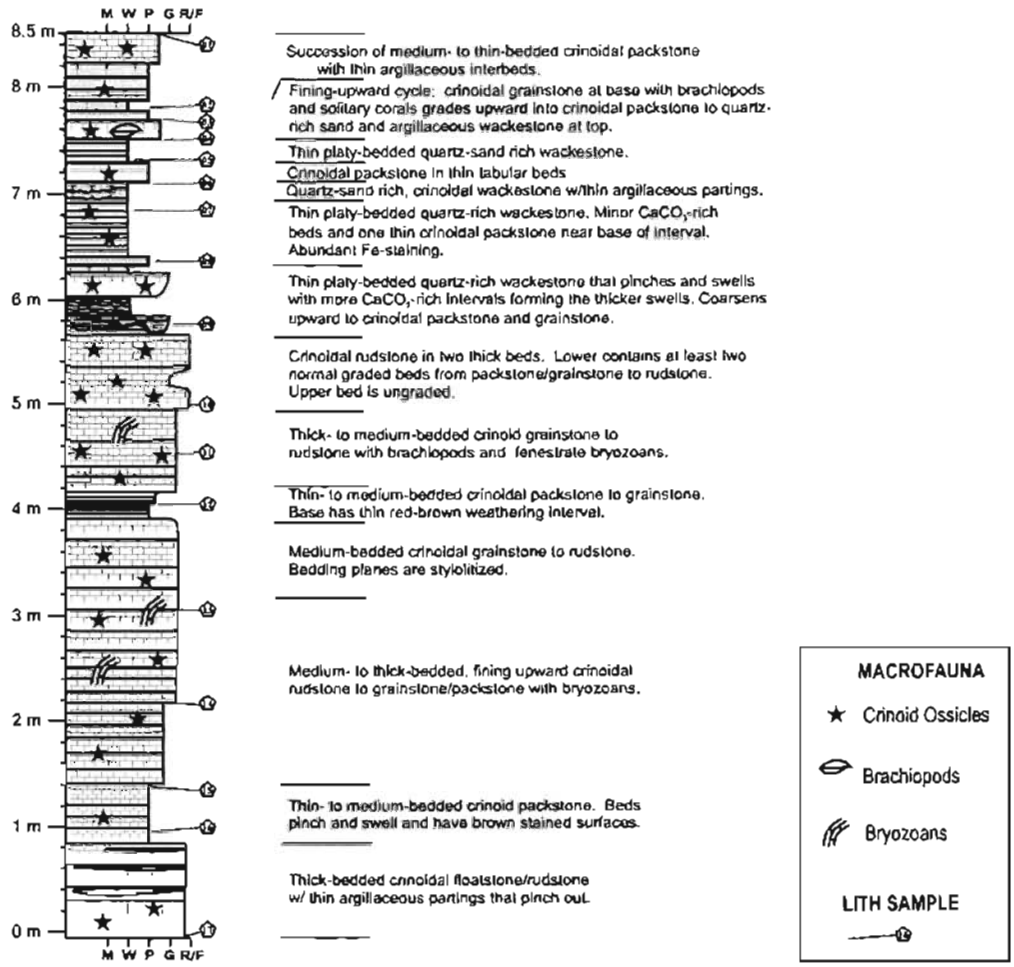

Stratigraphic section measured and described by J. Clough, M. Whalen, and R. Blodgett, June 1998.

LITHOLOGY: Thin- to thick-bedded limestone—predominantly crinoidal wackestone to packstone, grainstone, floatstone, and rudstone; and quartz-rich argillaceous platy limestone.

DEPOSITIONAL SETTING: Open marine carbonate platform environment with minor to significant terrigenous sediment influx. Abundant stenohaline fauna indicate open marine conditions during deposition. General lack of sedimentary structures suggests extensive burrowing activity and sedimentation within the oxygenated zone.

BIOSTRATIGRAPHIC DATA: Megafossil collection 97RB196 collected from rubble at the base of the section contains the following: numerous crinoid ossicles (both large and small), bryozoans (including fenestellids and polyporoids), limpet-like gastropod, trilobite pygidia, and abundant brachiopods. Brachiopods (identified by R.B. Blodgett) include: *Schizophoria* sp., *Waagenites* sp., echinoconchid, *Liosotella* aff. *hemisphaerica* Dunbar, *Kochiproductus*? sp., linoproductid, *Krotovia* sp., "*Camarophoria*" sp., Rhynchonellid, *Phricadothyris* sp., and *Spiriferellina cristata*? (Schlotheim). The megafossils were recovered from talus derived from the lower part (probably lowermost 2 m) of the cliff-like exposure at this locality. The brachiopod fauna is indicative of a Late Permian (Zechstein equivalent) age. A number of conodont samples were collected from the exposure at the following intervals: (1) 0.0–0.1 m, (2) 0.9–1.0 m, (3) 2.2–2.3 m, (4) 3.3–3.4 m, (5) 4.5 m, (6) 5.5 m, (7) 6.2–6.3 m, and (8) 7.3–7.4 m. All of the above were barren of conodonts, with the exception of the sample from 0.0–0.1 m which yielded 5 elements identified by N.M. Savage as *Hindeodus* sp. A generalized age call of Mississippian–Permian is indicated by the conodont collection.

Figure 13. *Upper Permian limestone section.*

as part of a Devonian ophiolite (Jones and others, 1980). The lower contact is interlayered with Upper Devonian (Famennian) radiolarian chert. The upper contact is difficult to discern, appears to be somewhat gradational, and may represent either an erosional unconformity or interfingering with overlying sedimentary rocks of unit PPs. Lower greenschist metamorphism is ubiquitous, as chlorite–albite–carbonate–epidote alteration of primary mafic and feldspar minerals. Immobile element compositions (fig. 10) indicate this unit formed as an intra-oceanic island arc. Compositional similarities to spatially associated gabbro blocks with serpentinite suggest that the units Dv, Dc, and sp represent different structural levels within an island arc.

Dc **Red and brown chert** (Upper Devonian) — Radiolarian chert, massive to well layered, predominantly red and brown, but also green and black. Locally manganiferous, with up to 0.5 percent MnO, and ferruginous. Radiolaria indicate a Late Devonian (Famennian) age. Found bedded in the lower portions of the Devonian tuff (unit Dv), but rarely of areal extent large enough to be mapped; also as large pods and blocks in fault zones, most notably in the drainage in southcentral portion of Sec. 16, T20S, R11W, where it occurs within serpentinite. Red chert clasts from this unit are found within conglomerate in unit TRvs.

Dl **Limestone** (Early? to Middle Devonian) — Medium- to thick-bedded, medium to dark gray lime mudstone to wackestone; locally fossiliferous with both rugose and tabulate corals, and brachiopods. Megafossils from the field area (loc. 114–116, Blodgett and Clautice, 2000), as well as equivalent exposures in the Reindeer Hills, Healy C-4 Quadrangle (Blodgett, 1977) indicate a Middle Devonian or slightly older age, although one locality in the field area yielded conodonts identified as being of Late Silurian (latest Pridolian) or Early Devonian (Gedinnian, or Lochkovian) age (Jones and others, 1980).

Rocks of unknown age

sp **Serpentinite gabbro and silica–carbonate rocks** — Mixed unit varying from intensely serpentinized, chromite-bearing dunite to altered gabbro (sheet 1, photo 7). Serpentinite is commonly altered to silica–carbonate rock and is otherwise strongly magnetic. Gabbro is commonly layered, and varies from fine- to coarse-grained and from leucocratic to melanocratic altered clinopyroxene–plagioclase rock. Plagioclase is ubiquitously altered to clinozoisite–albite–sericite and pyroxene to chlorite–carbonate–epidote. Major- and trace-element similarities of the gabbro to basaltic members of the Devonian(?) volcaniclastic unit (Dv) suggest that the gabbros were feeders for the Devonian volcanics. Generally occurs as tectonic lenses occupying the hinge zones of antiforms within Devonian (?) volcanic unit (Dv) and along faults separating unit Dv from unit TRvs. Devonian age suggested due to common spatial proximity with Devonian chert unit, but age is not well constrained.

sp* **Aeromagnetic high, probable serpentinite and gabbro** — This map unit is delineated by a narrow, strong magnetic signature that trends northeast through Broad Pass (sheet 1, aeromagnetic map). Serpentinite was found in three locations in this area of little bedrock exposure and at one locality near basalt with major- and trace-element similarities to unit Dv. This unit is believed to be very similar to unit sp above.

INTRUSIVE ROCKS

Tg **Biotite granite** (Eocene) — Textures range from fine-grained porphyritic (dikes) to coarse-grained, subequigranular. Normative compositions indicate most rocks are classified as alkali feldspar granite and lesser syeno–granite (fig. 12a). Locally altered to tourmaline–zinnwaldite ± biotite granite. Generally ilmenite series, lacking primary magnetite and sphene. Minor phases include topaz, zircon, apatite, and fluorite. $^{40}Ar/^{39}Ar$ dating of these rocks indicates a range in age from about 46 Ma to 55 Ma with most between about 50 and 55 Ma (table 1). Trace-element data (fig. 12b) indicate the rocks are highly fractionated members of collision- or extension-related felsic magmas. Narrow basaltic or lampropheric dikes (Tb) commonly intrude these bodies.

Tb **Basaltic-composition dikes** (Eocene) — Narrow (0.3 – 2 m wide), fine-grained, dark-colored, mafic dikes that cut Late Cretaceous granites. Most readily distinguished in the field by rare clinopyroxene phenocrysts, up to 2 cm in size, and by occurrence with Tertiary granite. Major and minor element compositions indicate these are exclusively of basalt composition, and some are alkali basalt (figs. 8b, 12). These rocks typically possess magnetic susceptibilities intermediate between those of units Trb and Km. Immobile element compositions indicate an extensional-related setting (fig. 10b); most likely they represent the mafic member of an early Tertiary bimodal magmatic suite. $^{40}Ar/^{39}Ar$ dating of one dike indicates an age of about 52 Ma (table 1).

Kg **Late Cretaceous (hornblende) biotite granite** — Monzo- and syeno-granite composition rocks (fig. 12a) with $^{40}Ar/^{39}Ar$ minimum ages (table 2) of about 61.4 to 71 Ma. On the west side of the Parks Highway these

are seen as dikes and small stocks with granite porphyry textures; on the east side as large bodies of sub-equigranular granite with grain sizes of 2 mm to 2 cm. These rocks appear to be compositionally and mineralogically transitional to Km, with no sharp compositional break between the two (fig. 12a). Modal abundances are typically 20—30 percent quartz, 30–40 percent plagioclase (An_{5-15}), 30–40 percent K-feldspar (chiefly orthoclase) and 5–10 percent biotite. Trace amounts of hornblende, zircon, apatite, and ilmenite are also present. Rocks of this unit commonly display moderate to extensive hydrothermal alteration: biotite to muscovite + chlorite + rutile and plagioclase to calcite + fine-grained white mica.

Unit Kg is distinguished with difficulty from Tg in the field, especially in the central part of the map area, where both occur as rhyolite porphyry dikes. Kg, however, characteristically lacks tourmaline, fluorite, and coarse-grained muscovite. In the southeast part of the map area, Kg typically occurs as texturally and mineralogically monotonous biotite granite, lacking appreciable chill, or pegmatite- or aplite-textured zones. Compositionally, rocks of unit Kg generally contain lower Rb and Nb + Y (fig. 12b) and higher normative anorthite (fig. 12a) than Tg. Trace-element contents suggest that unit Kg, like Km, is of an arc-related origin (fig. 12b).

Km **Intermediate composition plutonic rocks (Late Cretaceous)** — Bodies of Km range in size from small stocks to narrow dikes, typically oriented northeast–southwest. Rock textures vary considerably, from fine-grained porphyritic to medium-grained, sub-equigranular. The dominant mafic mineral is hornblende; biotite is common in more felsic, and clinopyroxene in more mafic, varieties. Minor to major chlorite–carbonate–sericite–albite–epidote–pyrite (propyllitic) alteration is common. Generally ilmenite series, that is, lacking primary magnetite and sphene. Minor phases include zircon, allanite, and apatite.

Compositions are dominantly quartz monzodiorite, but quartz diorite, quartz monzonite, and granodiorite are also present (fig. 12a). Despite their generally quartz-poor character, trace-element contents indicate a volcanic arc-related origin (fig. 12b). $^{40}Ar/^{39}Ar$ dating of these rocks and their hornfels zones (table 2) indicates a spread of ages from about 67 Ma to 71 Ma; some of the younger ages have been thermally reset and the true age spread is likely narrower. Most Km dikes are easily recognized in the field by their distinctive hornblende phenocrysts. Fine-grained and mafic varieties of Km are distinguished from mafic dikes of units Trb and Tb by distinctive immobile element contents (fig. 8b) and their lower magnetic susceptibilities. Similarities in age (about 70 Ma) as well as major and minor element compositions (Szumigala, 1993; McCoy and others, 1997) suggest that this igneous suite represents the same Late Cretaceous, intermediate composition magmatic event as the gold-related Kuskokwim Mountains magmatic belt of southwestern Alaska.

ACKNOWLEDGMENTS

C.C. Hawley shared his expertise on the geology, mineral deposits, and mining history of the Chulitna district in addition to providing accommodations. Several University of Alaska Fairbanks students contributed to the project: Sara Haug assisted in the field, Adam Low provided a report on existing literature and geophysical interpretations, Ben Gage and Paul Chu compiled geochemical data. Paleontologic work was under the direction of Robert Blodgett with assistance provided by M.Z. Won and Paula Noble (radiolarians); Chris McRoberts, Michael Sandy and George Stanley (Mesozoic megafossils); and Norman Savage (conodonts). Michael Whalen assisted with measuring the Permian limestone section. David Stone, with students Howard Scher and Chad Schopp, conducted paleomagnetic studies. Paul Layer, Deitre Hansen, Kaitlin Hansen, and Jeff Drake with the University of Alaska Geochronology Lab, performed $^{40}Ar/^{39}Ar$ geochronology. Paul Layer also provided considerable advice in interpretation of the Argon spectra. Mike Messing shared his mapping, photographs, and rock samples from the Honolulu Creek area. While all authors were involved in many aspects of the mapping project, special contributions were provided by Rainer Newberry (economic, structural and geologic interpretations, trace-element diagrams), Tom Bundtzen (Kahiltna rocks in the northwest map area), Ellen Harris (units Jac, uPzt, uPzst), Shirley Liss (units Jac, uPzt, Dv), Marti Miller (units TRvs, uPzt, uPzst), Rocky Reifenstuhl (units TRvs, KJs and Kahiltna rocks in the eastern map area), Jim Clough (units Pl and Tcs), and DeAnne Pinney (Quaternary and engineering geology and unit Ts). Review of this report was provided by Laurel Burns, Jeanine Schmidt, and Chuck Hawley and editing by Paula Davis.

Partial funding for this project was provided through U.S. Geological Survey STATEMAP Cooperative Agreement 98HQAG2083.

REFERENCES CITED

Alaska Division of Geological & Geophysical Surveys, Dighem and WGM, 1997a, 7200 Hz resistivity contours of the Chulitna mining district, Alaska: State of Alaska, Division of Geological & Geophysical Surveys Report of Investigations 97-4, 1 sheet, full color, scale 1:63,360.

———1997b, 900 Hz resistivity contours of the Chulitna mining district, Alaska: State of Alaska, Division of Geological & Geophysical Surveys Report of Investigations 97-3, 1 sheet, full color, scale 1:63,360.

———1997c, Total field magnetics and electromagnetic anomalies of the Chulitna mining district, Alaska: State of Alaska, Division of Geological & Geophysical Surveys Report of Investigations 97-1, 1 sheet, 3 colors, scale 1:63,360.

———1997d, Total field magnetics of the Chulitna mining district, Alaska: State of Alaska, Division of Geological & Geophysical Surveys Report of Investigations 97-2, 1 sheet, full color, scale 1:63,360.

Athey, J.E., 1999, Characterization of the DAT Zone, Eastern Alaska Range, Alaska: University of Alaska Fairbanks, unpublished M.S. Thesis, 137 p.

Balen, M.D., 1990, Geochemical sampling results from Bureau of Mines Investigations in the Valdez Creek mining district, Alaska: U.S. Bureau of Mines Open-File Report 34-90, 218 p.

Barker, Fred, Aleinikoff, J.N., Box, S.E., Evans, B.W., Gehrels, G.E., Hill, M.D., Irving, A.J., Kelley, J.S., Leeman, W.P., Lull, J.S., Nokleberg, W.J., Pallister, J.S., Patrick, B.E., Plafker, George, and Rubin, C.M., 1994, Some accreted volcanic rocks of Alaska and their elemental abundances, *in* Plafker, George, and Berg, H.C., eds., The geology of Alaska, the geology of North America: Boulder, Colorado, Geological Society of America, v. G-1, p. 555–587.

Barker, Fred, Sutherland Brown, A., Budahn, J.R., and Plafker, George, 1989. Back-arc with frontal-arc component of the Triassic Karmutsen Basalt, British Columbia, Canada: Chemical Geology, v. 75, p. 81102.

Beard, J.S., and Barker, Fred, 1989, Petrology and tectonic significance of gabbros, tonalites, shoshonites, and anorthosites in a Late Paleozoic arc-root complex in the Wrangellia terrane, southern Alaska: Journal of Geology, v. 97, p. 667–683.

Bhatia, M.R., 1983, Plate tectonics and geochemical composition of sandstones: Journal of Geology, v. 91, p. 611–627.

Blodgett, R.B., 1977, A Givetian (late Middle Devonian) fauna from Healy B-4 Quadrangle, central Alaska Range, Alaska, *in* Short Notes on Alaskan Geology–1977: Alaska Division of Geological & Geophysical Surveys, Geologic Report 55, p. 1–2.

Blodgett, R.B., and Clautice, K.H., 2000, Fossil locality map for the Healy A-6 Quadrangle, southcentral Alaska: Alaska Division of Geological & Geophysical Surveys Report of Investigations 2000-5, 42 p., 1 sheet, scale 1:63,360.

Brooks, A.H., and Prindle, L.M., 1911, The Mount McKinley region, Alaska; descriptions of the igneous rocks and of the Bonnifield and Kantishna districts: U.S. Geological Survey Professional Paper 70, p. 136–154, scale 1:625,000.

Burns, L.E., 1997, Portfolio of aeromagnetic and resistivity maps of the Chulitna mining district: Alaska Division of Geological & Geophysical Surveys Public-Data File Report 97-7, 13 p.

Capps, S.R., 1919, Mineral resources of the upper Chulitna region: U.S. Geological Survey Bulletin 692-D, p. 207–232.

———1940, Geology of the Alaska Railroad region: U.S. Geological Survey Bulletin 907, 201 p., scale 1:250,000.

Clark, A.L., Clark, S.H.B, and Hawley, C.C., 1972, Significance of upper Paleozoic oceanic crust in the upper Chulitna district, west-central Alaska Range: U.S. Geological Survey Professional Paper 800-C, p. C95–C101.

Clautice, K.H., Newberry, R.J., Blodgett, R.B., Bundtzen, T.K., Gage, B.G., Harris, E.E., Liss, S.A., Miller, M.L., Pinney, D.S., Reifenstuhl, R.R., Clough, J.G., Stone, D.B., and Whalen, M.T., 1999a, Preliminary geologic map of the Healy A-6 Quadrangle, southcentral Alaska: Alaska Division of Geological & Geophysical Surveys Public-Data File 99-24a, 28 p., 1 sheet, scale 1:63,360.

Clautice, K.H., Newberry, R.J., Blodgett, R.B., Bundtzen, T.K., Gage, B.G., Harris, E.E., Liss, S.A., Miller, M.L., Reifenstuhl, R.R., Clough, Pinney, D.S., J.G., Stone, D.B., and Whalen, M.T., 1999b, Preliminary interpretive bedrock geologic map of the Healy A-6 Quadrangle, southcentral Alaska: Alaska Division of Geological & Geophysical Surveys Public-Data File 99-24b, 26 p., 1 sheet, scale 1:63,360.

Csejtey, Béla, Jr., Cox, D.P., Evarts, R.C., Stricker, G.D., and Foster, H.L., 1982, The Cenozoic Denali fault system and the Cretaceous accretionary development of southern Alaska: Journal of Geophysical Research, v. 87, no. B5, p 3,741-3,754.

Csejtey, Béla, Jr., Mullen, M.W., Cox, D.P., and Stricker, G.D., 1992, Geology and geochronology of the Healy Quadrangle, south-central Alaska: U.S. Geological Survey Map I-1961, 63 p., scale 1:250,000, 2 sheets.

Csejtey, Béla, Jr., Nelson, W.H., Jones, D.L., Silberling, N.J., Dean, R.M., Morris, M.S., Lanphere, M.A., Smith, J.G., and Silberman, M.L., 1978, Reconnaissance geologic map and geochronology, Talkeetna Mountains quadrangle, northern part of Anchorage quadrangle, and southwest corner of Healy quadrangle,

Alaska: U.S. Geological Survey Open-File Report 78-558A, 62 p., scale 1:250,000.

Davis, Alice, and Plafker, George, 1985, Comparative geochemistry and petrology of Triassic basaltic rocks from the Taku Terrane on the Chilkat Peninsula and Wrangellia: Canadian Journal of Earth Sciences, v. 22, p. 183–194.

Eastham, K.R, Ridgway, K.D., and Lesh, M.E., 2000, Structural configuration and stratigraphy of the Kahiltna basin(s): A detailed look at the 'Black Crap' of central Alaska (abstract), *in* Summit 2000, Geological Society of America Annual Meeting, Reno, Nevada, Nov 9–18, 2000, Abstracts with Programs, v. 32, no. 7, p. A171.

Fryda, J., and Blodgett, R.B., 2001, *Chulitnacula*, a new paleobiogeographically distinctive gastropod genus from Upper Triassic strata in accreted terranes of southern Alaska: Journal of Czech Geological Society, v. 46, nos. 3–4, p. 213-220.

Gage, B.G., Chu, P.S., Liss, S.A., and Clautice, K.H., 1998, Preliminary geochemical and major oxide data: Chulitna project, Healy A-6 Quadrangle and nearby areas (1997 & 1998 data): Alaska Division of Geological & Geophysical Surveys Public-Data File 98-36a, 48 p., 2 sheets, scale 1:63,360, 1 disk.

Hart, C.J.R., 1997, A transect across northern Stikinia: geology of the northern Whitehorse map area, southern Yukon Territory: Yukon, Exploration and Geological Services Division, Indian and Northern Affairs Canada, Bulletin 8, 112 p.

Hawley, C.C., and Clark, Allen L., 1973, Geology and mineral deposits of the Chulitna–Yentna Mineral Belt, Alaska: U.S. Geological Survey Professional Paper 758-A, p. A1–A10, 2 sheets, scales 1:250,000, 1:500,000.

———1974, Geology and mineral deposits of the Upper Chulitna district, Alaska: U.S. Geological Survey Professional Paper 758-B, p. B1–B47, scales 1:48,000, 1:24,000, 1:12,000.

Hawley, C.C., Clark, A.L., and Benfer, J.A., 1968, Geology of the Golden Zone mine area, Alaska: U.S. Geological Survey Open-File Report 68–122 (305), 16 p., 1:2,400 scale.

Hawley, C.C., Clark, A.L., Herdrick, M.A., Clark, S.H.B., 1969, Results of geological and geochemical investigations in an area northwest of the Chulitna River, central Alaska Range: U.S. Geological Survey Circular 617, 19 p.

Hopkins, D.M., 1951, Lignite deposits near Broad Pass station, Alaska, *in* Barnes, F.F., Wahrhaftig, Clyde, Hickcox, C.A., Freedman, Jacob, and Hopkins, D.M., eds., Coal investigations in south-central Alaska, 1944–46: U.S. Geological Survey Bulletin 963-E, p. 187–191.

Jones, D.L., Silberling, N.J., Csejtey, Béla, Jr., Nelson, W.H., and Blome, C.D., 1980, Age and structural significance of ophiolite and adjoining rocks in the upper Chulitna district, south-central Alaska: U.S. Geological Survey Professional Paper 1121-A, p. A1–A21, 2 plates in text, 1 sheet, scale 1:63,360.

Jones, D.L., Silberling, N.J., Berg, H.C., and Plafker, George, 1981, Map showing tectonostratigraphic terranes of Alaska, columnar sections and summary description of terranes: U.S. Geological Survey Open-File Report 81-792, 20 p., 2 sheets, scale 1:2,500,000.

Kurtak, J.M., Southworth, D.D., Balen, M.D., and Clautice, K.H., 1992, Mineral investigations in the Valdez Creek mining district, south-central Alaska: U.S. Bureau of Mines OFR 1-92, 658 p.

Layer, P.W., Hall, C.M., and York, Derek, 1987, The derivation of $^{40}Ar/^{39}Ar$ age spectra of single grains of hornblende and biotite by laser step-heating: Geophysical Research Letters, v. 14, p. 757–760.

Light, T.D., Tripp, R.B., and King, H.D., 1990, Interpretation of reconnaissance geochemical data from the Healy quadrangle, Alaska: U.S. Geological Survey Bulletin 1894, 36 p.

MacKevett, E.M., Jr., Cox, D.P., Potter, R.W., and Silberman, M.L., 1997, Kennecott-type deposits in the Wrangell Mountains, Alaska: High-grade copper ores near a basalt–limestone contact, in Goldfarb, R.J., and Miller, L.D., eds., Mineral Deposits of Alaska: Economic Geology Monograph 9, p. 66–89.

Mason, Brian, 1966, Principles of Geochemistry (3rd edition): New York, John Wiley & Sons, 329 p.

McCoy, Dan, Newberry, R.J., Layer, P.W., DiMarchi, J.J., Bakke, A.A., Masterman, J.S., and Minehane, D.L., 1997, Plutonic-related gold deposits of Interior Alaska, *in* Goldfarb, R.J., and Miller, L.D., eds., Mineral Deposits of Alaska: Economic Geology Monograph 9, p. 191–241.

Meinert, L.D., 1992, Skarns and skarn deposits: Geoscience Canada, v. 19, p. 145–162.

Merritt, R.D., and Hawley, C.C., 1986, Map of Alaska's coal resources: Alaska Division of Geological & Geophysical Surveys Special Report 37, 1 sheet, scale 1:2,500,000.

Moffit, F.H., 1915, The Broad Pass region, Alaska, with sections on Quaternary deposits, igneous rocks, and glaciation by J.E. Pogue: U.S. Geological Survey Bulletin 608, 80 p., scale 1:250,000.

Montayne, Simone, and Whalen, M.T., in press, Permian cool-water limestones from the Chulitna Terrane, southcentral Alaska, *in* Clautice, K.H., and Davis, P.K., Alaska Division of Geological & Geophysical Surveys, Short Notes on Alaska Geology 2001.

Mulligan, J.J., Warfield, R.S., and Wells, R.R., 1967, Sampling a gold–copper deposit, Golden Zone mine, south-central Alaska: U.S. Bureau of Mines open file report 9-67, 59 p.

Mutti, E. and Ricci Lucchi, F., 1978, Turbidites of the northern Appennines: Introduction to facies analysis: International Geology Review, v. 20, no. 2, p. 125–166.

Newberry, R.J., 1995, An update on skarn deposits of Alaska: Alaska Division of Geological & Geophysical Surveys, Public-data File 95-20, 87 p.

Newberry, R.J. and Solie, D.N., 1995, Data for plutonic rocks and associated gold deposits in Interior Alaska: Alaska Division of Geological & Geophysical Surveys Public-data File 95-25, 62 p.

Newberry, R.J., Allegro, G.L., Cutler, S.E., Hagen-Levelle, J.H., Adams, D.D., Nicholson, L.C., Weglarz, T.B., Bakke, A.A., Clautice, K.H., Coulter, G.A., Ford, M.J., Myers, G.L., and Szumigala, D.J., 1997, Skarn Deposits of Alaska, *in* Goldfarb, R.J., and Miller, L.D., eds., Mineral Deposits of Alaska: Economic Geology Monograph 9, p. 355–395.

Nichols, K.M., and Silberling, N.J., 1979, Early Triassic (Smithian) ammonites of paleoequatorial affinity from the Chulitna terrane, south-central Alaska: U.S. Geological Survey Professional Paper 1121-B, 5 p.

Nokleberg, W.J., Plafker, George, and Wilson, F.H., 1994, Geology of south-central Alaska, *in* Plafker, George, and Berg, H.C., eds., The Geology of North America, The Geology of Alaska: Geological Society of America, v. G-1, p. 311–366.

Parker, Tracey V.L., 1991, Mineralization in the Coal Creek tin prospect, south-central Alaska: U.S. Bureau of Mines field report, unpublished, 2 cross sections and 36 p.

Pearce, J.A., and Cann, J.R., 1973, Tectonic setting of basic volcanic rocks determined using trace element analyses: Earth and Planetary Science Letters, v. 19, p. 290–300.

Pearce, J.A., Harris, N.B.W., and Tindle, A.G, 1984, Trace element discrimination diagrams for the tectonic interpretation of granitic rocks: Journal of Petrology, v. 25, p. 956–983.

Pinney, D.S., 1999a, Reconnaissance engineering geologic map of the Healy A-6 Quadrangle, southcentral Alaska: Alaska Division of Geological & Geophysical Surveys Public-Data File 99-24d, 4 p., 1 sheet, scale 1:63,360.

———1999b, Reconnaissance surficial geologic map of the Healy A-6 Quadrangle, southcentral Alaska: Alaska Division of Geological & Geophysical Surveys Public-Data File 99-24c, 3 p., 1 sheet, scale 1:63,360.

Plafker, George, and Berg, H.C., editors, 1994, The Geology of Alaska, Decade of North American Geology, Volume G-1, Geological Society of America, 1055 p.

Reed, B.L., and Nelson, S.W., 1980, Geologic map of the Talkeetna quadrangle, Alaska: U.S. Geological Survey Miscellaneous Investigations Series Map I-1174, scale 1:250,000.

Richards, M.A., Jones, D.L., Duncan, R.A., and DePaolo, D.J. 1991, A mantle plume initiation model for the Wrangellia flood basalt and other oceanic plateaus: Science, v. 254, p.263–267.

Ross, C.P., 1933, Mineral deposits near the West Fork of the Chulitna River, Alaska: U.S. Geological Survey Bulletin 849-E, p. 289–333, 1 sheet, scale 1:125,000.

Samson, S.D., and Alexander, E.C., 1987, Calibration of the interlaboratory ^{40}Ar-^{39}Ar dating standard, MMhb-1: Chemical Geology, v. 66, p. 27–34.

Stanley, G.D. and Yarnell, J.M., in press, New paleontological investigations of Triassic carbonate rocks in the upper Chulitna district (Chulitna terrane), southcentral Alaska, *in* Clautice, K.H., and Davis, P.K., eds., Short Notes on Alaska Geology 2001: Alaska Division of Geological & Geophysical Surveys.

Steiger, R.H. and Jaeger, E., 1977, Subcommission on geochronology: Convention on the use of decay constants in geo and cosmochronology: Earth and Planetary Science Letters, v. 36, p. 359–362.

Stone, D.B., Scher, Howard, and Schopp, Chad, 1999, Chulitna-area paleomagnetic studies: Alaska Division of Geological & Geophysical Surveys Raw-Data File 1999-2, 4 p.

Streckeisen, A.L., and LeMaitre, R.W., 1979, A chemical approximation to the modal QAPF classification of the igneous rocks: Neues Jahrbuch fur Mineralogie Abhandlungen, v. 136, p. 169–206.

Swainbank, R.C., Smith, T.E., and Turner, D.L., 1977, Geology and K-Ar age of mineralized intrusive rocks from the Chulitna mining district, central Alaska, *in* Short notes on Alaskan Geology—1977: Alaska Division of Geological & Geophysical Surveys, Geologic Report 55, p. 23–28.

Szumigala, D.J., 1993, Gold mineralization related to Cretaceous–Tertiary magmatism in the Kuskokwim Mountains of west-central and southwestern Alaska: Los Angeles, California, University of California, unpublished Ph.D. dissertation, 301 p.

Wahrhaftig, Clyde, 1944, Coal deposits of the Costello Creek basin, Alaska: U.S. Geological Survey Open-File Report 8, 7 p., 6 sheets.

Wahrhaftig, Clyde, and Black, R.F., 1958, Engineering geology along part of the Alaska Railroad: U.S. Geological Survey Professional Paper 293-B, p. 79–118, 6 sheets, scale 1:63,360.

Warner, J.D., and Dahlin, D., 1989, Tin occurrences associated with the Ohio Creek pluton, Chulitna region, south-central Alaska: U.S. Bureau of Mines Open-File Report 5-89, 29 p.

Winchester, J.A. and Floyd, P.A., 1977, Geochemical discrimination of different magma series and their differentiation products using immobile elements: Chemical Geology, vol. 20, p. 325–343.

Won, M.Z., Blodgett, R.B., Clautice, K.H., and Newberry, R.J., 2000, Late Devonian (late Famennian) radiolarians from the Chulitna terrane, southcentral Alaska, in Pinney, D.S., and Davis, P.K., eds., Short Notes on Alaska Geology 1999: Alaska Division of Geological & Geophysical Surveys Professional Report 119, p. 145-152.